NASA Technical Memorandum 105273

Hydrogen No-Vent Fill Testing in a 1.2 Cubic Foot (34 Liter) Tank

Matthew E. Moran and Ted W. Nyland
Lewis Research Center
Cleveland, Ohio

and

Susan L. Driscoll
Marshall Space Flight Center
Huntsville, Alabama

October 1991

NASA

HYDROGEN NO-VENT FILL TESTING IN A 1.2 CUBIC FOOT (34 LITER) TANK

Matthew E. Moran, Ted W. Nyland
National Aeronautics and Space Administration
Lewis Research Center
Cleveland, Ohio 44135

and

Susan L. Driscoll
National Aeronautics and Space Administration
Marshall Space Flight Center
Huntsville, Alabama 35812

ABSTRACT

Experimental results of no-vent fill testing with liquid hydrogen in a 1.2 cubic foot (34 liter) stainless steel tank are presented. More than 40 tests were performed with various liquid inlet temperatures, inlet flowrates, initial tank wall temperatures, and liquid injection techniques. Fill levels equal to or exceeding 90 percent by volume were achieved in 40 percent of the tests with the tank pressure limited to a maximum of 30 psia. Three liquid injection techniques were employed; top spray, upward pipe discharge, and bottom diffuser. Effects of each of the varied parameters on the tank pressure history and final fill level are evaluated. The final fill level is found to be indirectly proportional to the initial wall and inlet liquid temperatures and directly proportional to the inlet liquid flowrate. Furthermore, the top spray is the most efficient no-vent fill method of the three configurations examined. The success of this injection method is primarily due to condensation of the ullage vapor onto the incoming liquid droplets. Ullage condensation counteracts the tank pressure rise resulting from energy exchange between the fluid and the warmer tank walls, and ullage compression. Upward pipe discharge from the tank bottom is the next most efficient method. Fluid circulation induced by this fill configuration tends to diminish thermal stratification in the bulk liquid, thus enhancing condensation at the liquid-gas interface.

INTRODUCTION

The test series described in this paper is part of an ongoing effort to advance cryogenic fluid handling technologies for space based applications. The ground test program being conducted by

the Cryogenic Fluids Technology Office of the NASA Lewis Research Center (LeRC) is focused on proof-of-concept demonstration as well as verification of analytical models which simulate key cryogenic fluid handling processes.

One of these key processes is the transfer of liquid hydrogen between tanks using the no-vent fill technique. This technique involves chilling the receiver tank to a predetermined average wall temperature and then filling the tank without venting. The no-vent fill method is well suited to microgravity cryogen handling since it eliminates the need for tank venting during the fill process. Venting of a tank in a microgravity environment risks substantial loss of cryogen due to the uncertain positioning of liquid and vapor within the tank.

No-vent fill testing with both nitrogen and hydrogen has been performed at the LeRC Cryogenic Components Laboratory, Cell 7 (CCL-7). Preliminary results of earlier testing with a 5 cubic foot receiver tank have been reported (Ref. 1). This paper discusses a more extensive array of test runs recently completed with a smaller, 1.2 cubic foot receiver tank. These tests incorporate three different liquid injection techniques; top spray, upward pipe discharge, and bottom diffuser. The fill technique used dictates the heat and mass transfer process which takes place at the liquid-vapor interface. As a result, each of these configurations generates a unique tank pressure profile during the fill process.

EXPERIMENTAL RIG DESCRIPTION

A photograph of the CCL-7 test rig is shown in Fig. 1. Operation and monitoring functions are performed in a remotely located control room, which is separated from the testing area by earth embankments. Video cameras provide continuous viewing of the rig from several nearby vantage points. The facility is designed to accommodate both nitrogen and hydrogen testing. A detailed description of the test rig and its operation is given in Ref. 1.

Tanks and Piping

Fluid handling tests in the CCL-7 facility are performed with a supply dewar and two interchangeable receiver dewars. The supply dewar is a vacuum jacketed stainless steel tank that contains multi-layer insulation (MLI) within the vacuum annulus. The dewar is cylindrical, with an internal height of 54 inches and an inside diameter of 22 inches. Internal volume of the supply tank is approximately 10.8 cubic feet.

The receiver dewars are of similar construction as the supply dewar. The large receiver, with an

internal height of 28 inches and an inside diameter of 22 inches, has an internal volume of approximately 5.0 cubic feet. The small receiver has an internal height of 20 inches and inside diameter of 12.5 inches, resulting in an internal volume of 1.2 cubic feet. The lids of both receiver tanks are composed of a flat flange which supports a short cylindrical section with an inverted dome bottom. The space between the flange and cylindrical section is evacuated and insulated with MLI to minimize heat transmission through the dome from the environment. With the lid in place, the interior walls of the assembled receiver tanks form a cylindrical storage volume with domed ends. Fig. 2 presents a photograph of the small receiver lid.

Heat transfer from the environment is a function of liquid fill level for the supply and receiver tanks. This is due to the disproportionate heat flux entering from the tank top as a result of various lid mounted penetrations and the coupling of the lid walls to ambient temperatures at the tank flange. The overall heat flux for all three tanks was experimentally determined, and ranges from 1 to 10 Btu/hr·ft^2 depending on the fill level and test fluid (nitrogen or hydrogen).

ORIGINAL PAGE
BLACK AND WHITE PHOTOGRAPH

Fig. 1: Photograph of the CCL-7 test cell

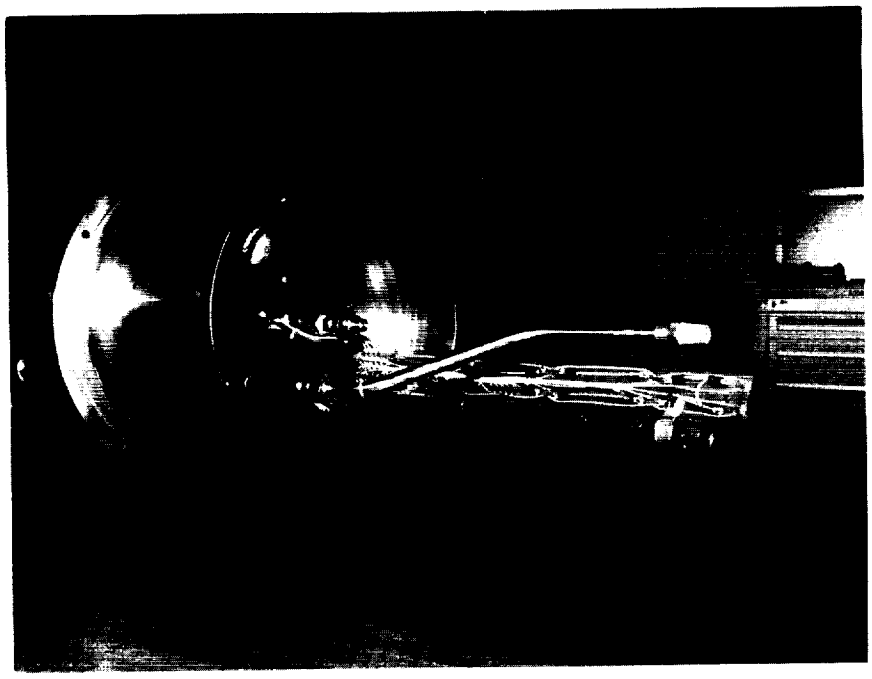

Fig. 2: Photograph of the small receiver lid assembly.

Liquid transfer lines are constructed of stainless steel, and vacuum jacketed or foam insulated throughout the rig. The rig is capable of transferring liquid cryogen between all of the dewars using a variety of fill configurations. The vent system is composed of stainless steel lines connected to each tank. An air ejector system provides sub-atmospheric pressure control in the vent lines to as low as 2 psia. Pressurization with helium, hydrogen, or nitrogen, is available for the supply and receiver tanks. A simplified piping schematic of the test rig is given in Fig. 3.

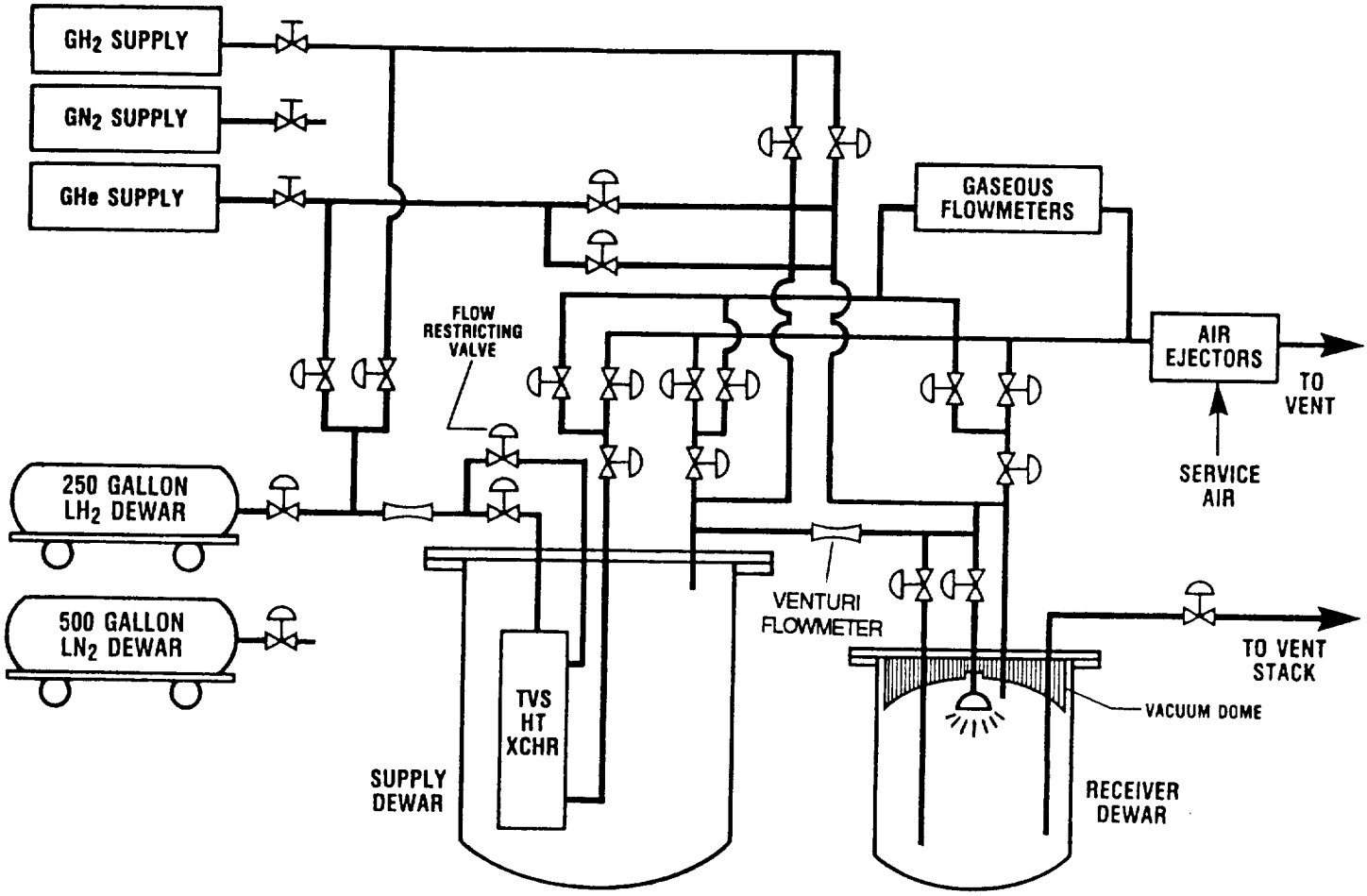

Fig. 3: Simplified piping schematic of CCL-7 test rig

Instrumentation and Data Acquisition

Temperature sensors are positioned throughout the rig and on the tank walls, selected fluid lines, and components. Temperatures are measured with type T (copper-constantan) thermocouples and silicon diodes, and thermistors are utilized to indicate the presence of liquid or vapor. Tank wall sensors are located in the annular vacuum space of the supply and receiver tanks, and are mounted to the inner tank wall. Within each tank is an instrument tree with silicon diodes and thermistors attached at various heights. This tree is in direct contact with the tank contents, whether liquid or vapor. Silicon diode sensors are accurate to within ± 0.2 °R, whereas, the thermocouples are accurate to within ± 2 °R. Fig. 4 illustrates temperature sensor and thermistor locations for the supply and small receiver tanks.

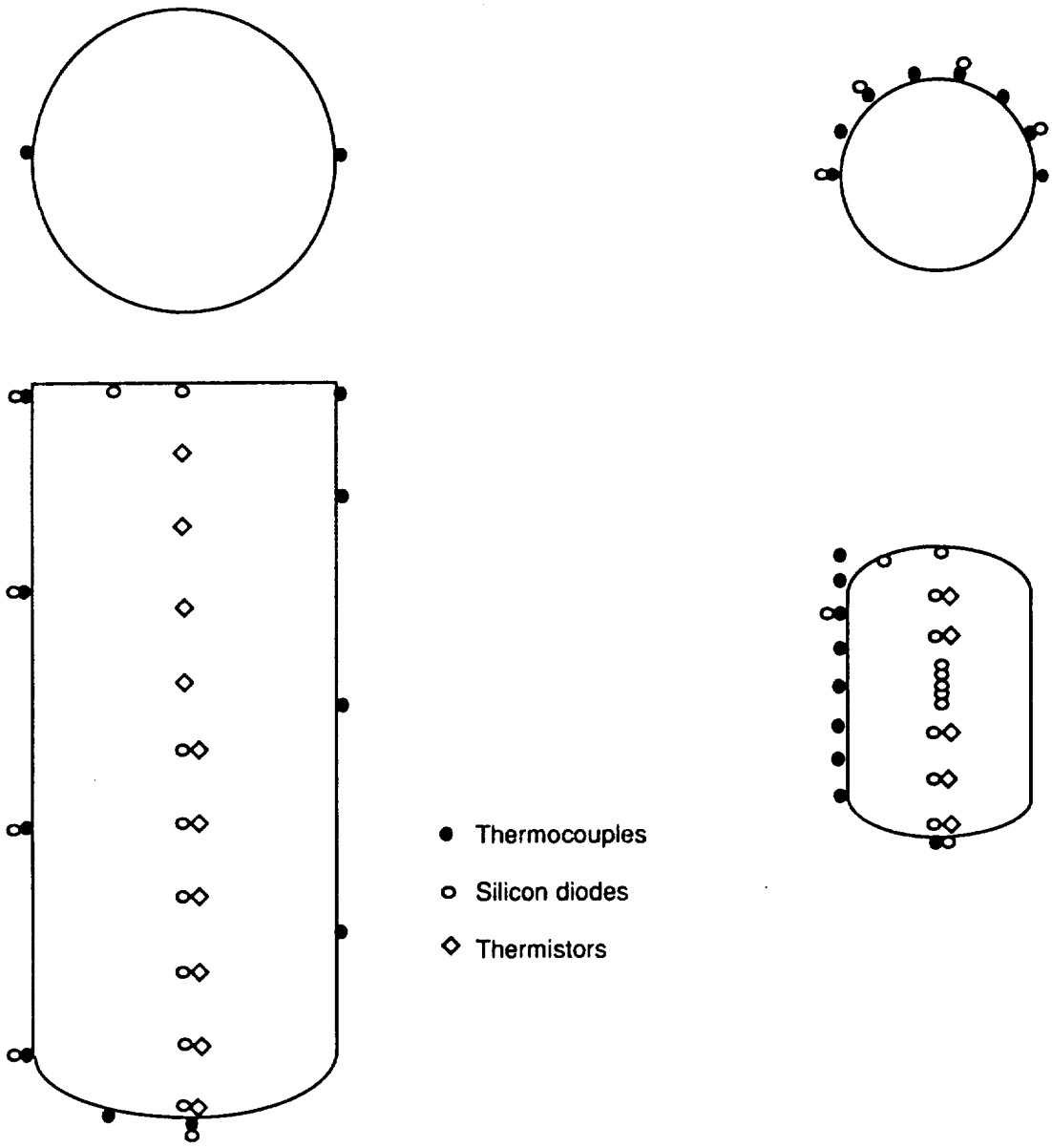

Fig. 4: Approximate locations of temperature sensors and thermistors for the supply and small receiver tanks.

Transducers provide continuous pressure measurement throughout the system with an estimated accuracy of ± 0.5 percent. Each tank is equipped with a capacitance type level probe which is used to calculate the liquid fill level. The level probe in the small receiver tank was calibrated in liquid

hydrogen against point sensors (thermistors) and found to agree within one inch for liquid levels greater than 10 percent.

Data acquisition is controlled by the microcomputer with software written in the C programming language. Nominally, 240 channels of data are taken on the test rig. The data acquisition software also controls data display for control panel indicators and the CRT monitor of the microcomputer. Toggle switches, selector knobs, and continuously adjustable dials mounted on the control panel are used to control the system valves and fluid routing.

TEST PROCEDURE

Performance of a no-vent fill test at CCL-7 involves five sequential steps. First, the system is pressurized to 25 psia with gaseous helium and checked for leaks. The helium is then vented through the air ejectors. This purge cycle is repeated a total of four times. Second, the supply dewar is filled from the roadable dewar with enough liquid to perform the planned test. With the supply tank filled, the liquid is thermally conditioned by controlling the tank pressure with the air ejector system. Third, with the cryogen conditioned to the desired temperature, the supply tank is pressurized for liquid transfer. The transfer line and associated components (e.g. valves, fittings, etc.) are then prechilled with a low flowrate of liquid. In the fourth step, the receiver tank pressure is reduced below atmospheric with the air ejectors. A charge of liquid is then loaded into the receiver tank with the vent valve closed. The vent remains closed while the liquid vaporizes, thus removing heat from the tank walls. When the tank pressure reaches a predetermined maximum or stabilizes, the vent valve is opened. Additional cooling is achieved as the tank pressure is once again brought below one atmosphere using the air ejector system. The resulting charge-hold-vent cycle is repeated until the tank wall temperature is reduced to the desired starting condition. In the fifth and final step, the liquid cryogen is transferred from the supply to the receiver tank with the vent valve closed until the receiver is filled to the desired level or until the pressure reaches a predetermined maximum value.

RESULTS AND DISCUSSION

A total of 42 no-vent fills were performed with the small, 34 liter receiver tank: 19 top spray, 7 upward pipe discharge, and 16 bottom diffuser tests. Fig. 5 illustrates the three fill configurations tested.

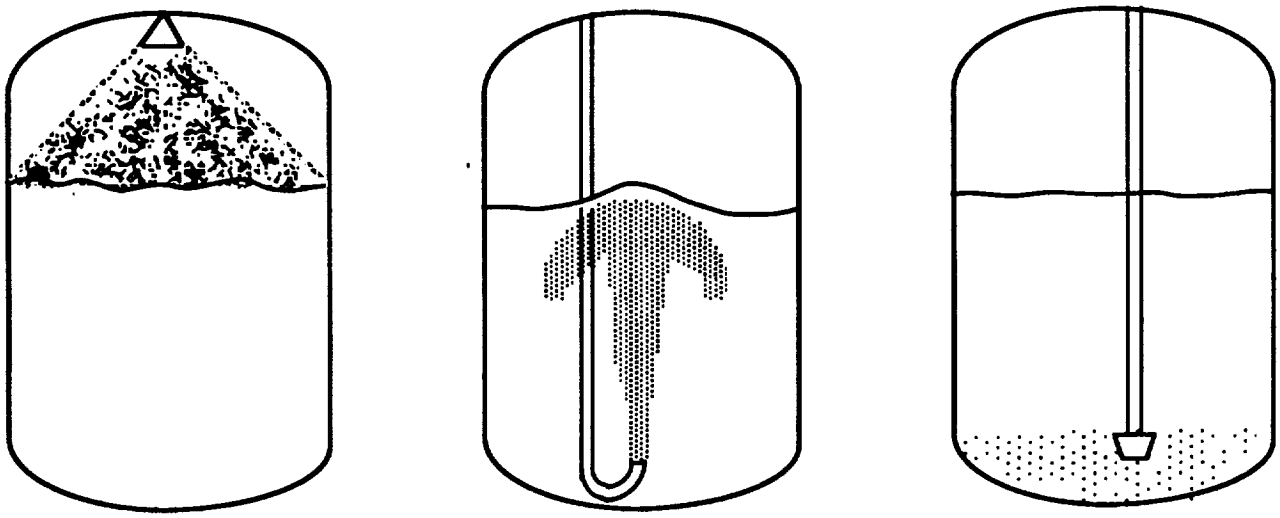

Top Spray Upward Pipe Discharge Bottom Diffuser

Fig. 5: Fill configurations used for no-vent fills in CCL-7.

Characterization of Fill Configurations

Top spray. A typical pressure history plot for one of the top spray fills is shown in Fig. 6. Three distinguishable pressure response regions are denoted by dashed lines. These regions are consistent with the pressure histories documented with earlier tests using a top spray in the large receiver tank (see ref. 1). In region 1, the incoming liquid flashes as it enters the low pressure tank and impinges on the warm tank walls. This results in a rapid rise in the tank pressure. As the

walls cool down, and the saturation pressure corresponding to the inlet liquid temperature is approached, the pressure history curve transitions into region 2. In region 2, vaporization of the liquid cryogen decreases, and the effect of ullage gas condensation onto the incoming liquid droplets becomes more evident. The magnitude and sign of the pressure curve slope in region 2 is dictated by the competing processes of condensation, ullage compression, and vaporization within the tank. Finally, in region 3, the pressure begins to rise sharply as the spray nozzle starts to become submerged by the rising liquid interface. As the nozzle is covered, condensation on the liquid droplets ceases and the ullage is compressed.

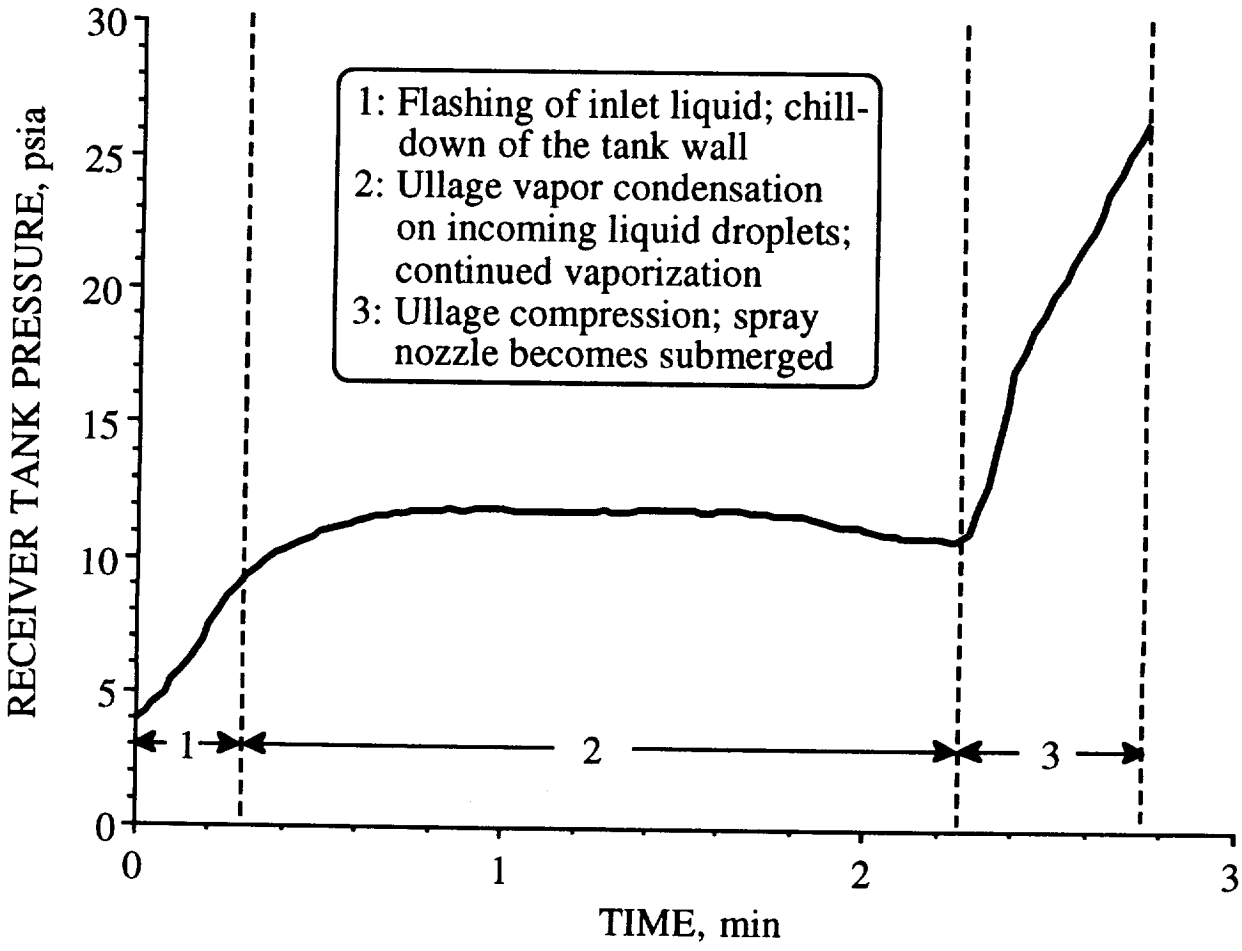

Fig. 6: Tank pressure as a function of time for a hydrogen no-vent fill test using the top spray fill configuration (9093A).

A plot of the liquid fill level in the tank as a function of time (Fig. 7) indicates a reasonably steady mass flow rate into the tank. Variation in the flow rate occurs during the beginning and end portions of the tests, however, as indicated by a change in slope of the liquid level plot. At the start of the test, vaporization of the incoming droplets results in a nearly constant fill level during the first ten seconds. Also, the flowrate drops off toward the end of the test as the receiving tank pressure approaches that of the supply tank.

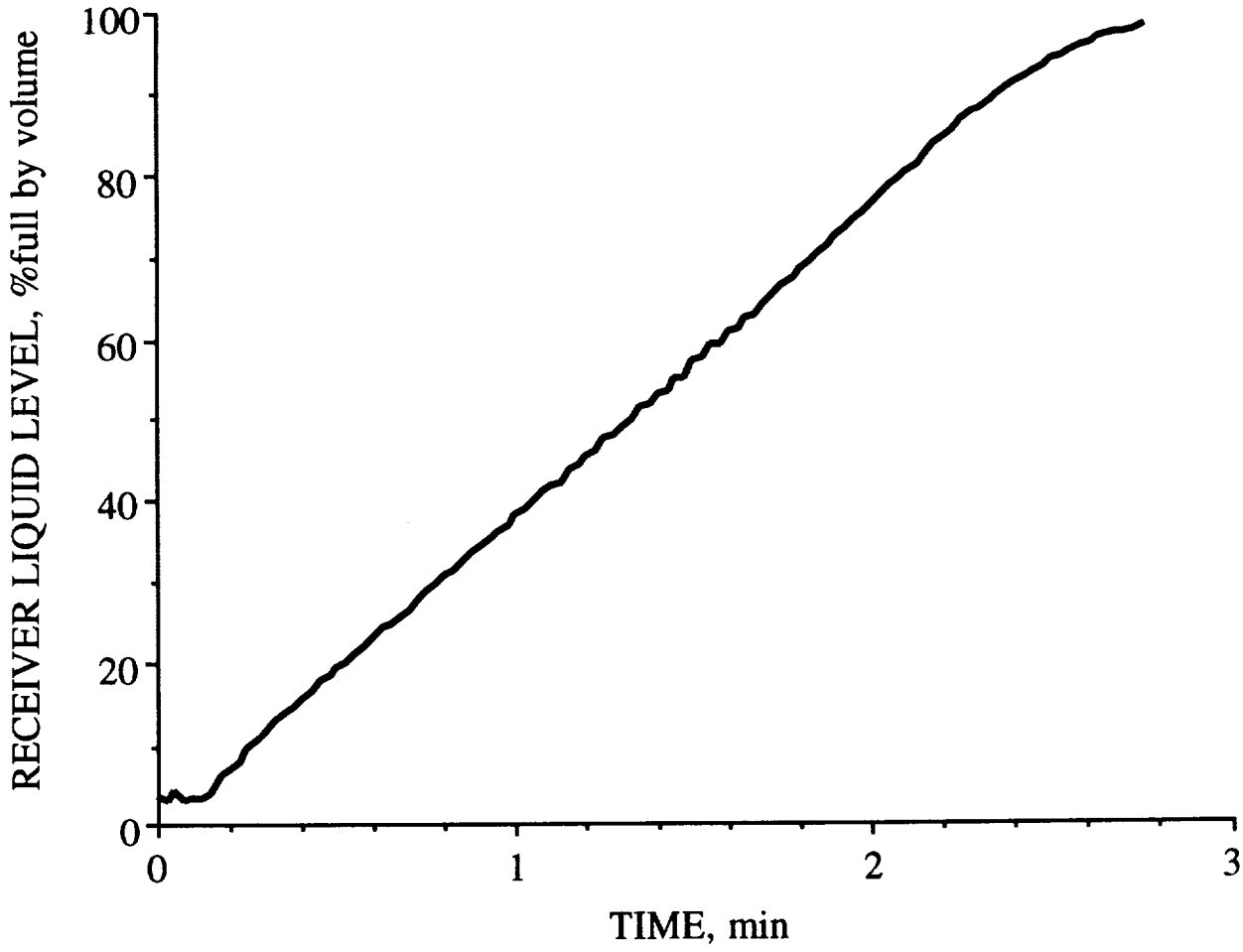

Fig. 7: Liquid fill level as a function of time for a hydrogen no-vent fill test using the top spray fill configuration (9093A).

Fig. 8 displays the internal tank temperatures recorded by the instrument tree during the same no-vent fill. All of the tree temperatures drop rapidly as the inlet spray fills the tank volume. This

behavior is consistent with previous no-vent fill tests performed with the large receiver tank using the top spray configuration.

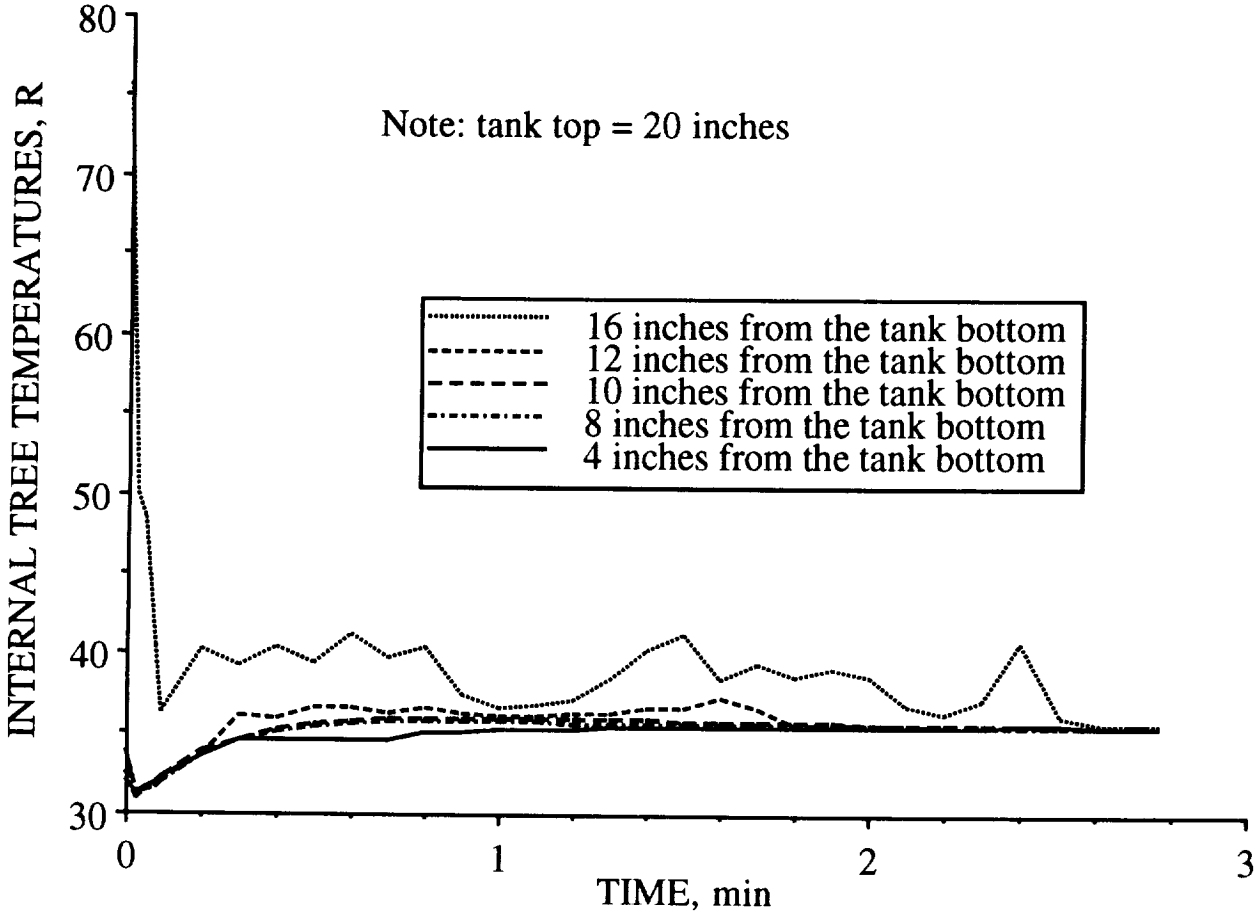

Fig. 8: Internal tree temperatures as a function of time for a hydrogen no-vent fill test using the top spray fill configuration (9093A).

Tank wall temperatures for this test are shown in Fig. 9. Some of the wall sensor positions have been omitted from this plot for clarity. All sensors except the top one remain at liquid hydrogen temperatures throughout the run. The top sensor, which is not exposed to the inlet liquid spray, cools gradually over most of the test run. Toward the latter portion of the test, the top sensor rises in temperature as the remaining tank ullage is compressed and the spray nozzle becomes submerged.

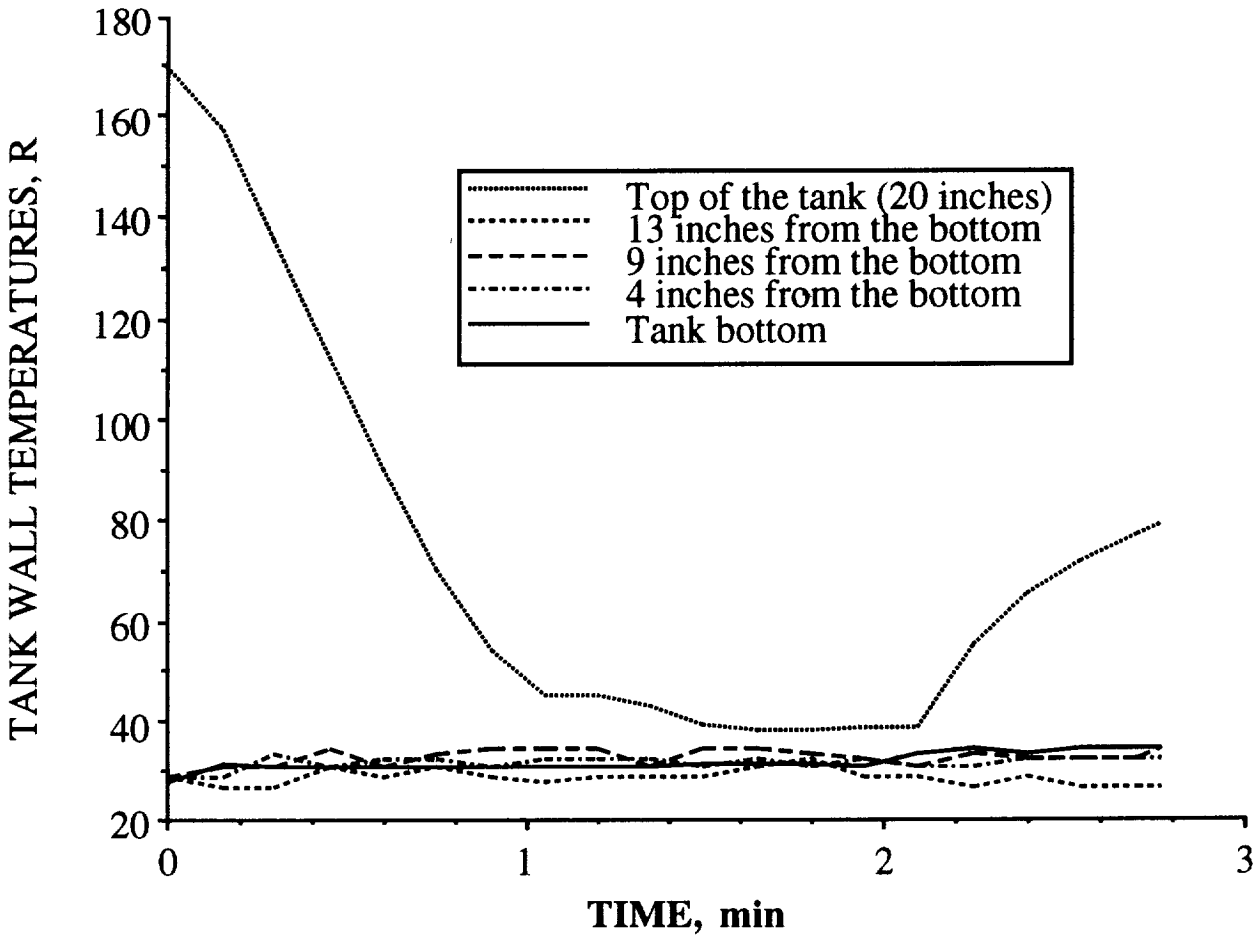

Fig. 9: Tank wall temperatures as a function of time for a hydrogen no-vent fill test using the top spray fill configuration (9093A).

Upward pipe discharge. A pressure history plot for one of the upward pipe discharge no-vent fills is given in Fig. 10. As with the top spray configuration, the pressure response curve displays three distinguishable regions. In region 1, the pressure rises sharply as the liquid enters the low pressure tank and flashes. However, this initial pressure rise is less dramatic for the upward pipe discharge configuration. Region 2 is characterized by a gradual increase in tank pressure as the liquid level rises in the tank. Condensation at the liquid-vapor interface is enhanced due to fluid circulation induced by the upward liquid motion. This circulation reduces the thermal stratification within the bulk liquid and brings the cooler fluid to the interface. Lastly, an increase in the slope of the pressure curve is evident in region 3 as the effect of ullage compression becomes more pronounced, and the liquid interface rises into the upper dome region. Once again, the pressure

rise in region 3 is less dramatic than for the spray configuration since the condensation process is not altered significantly (i.e. as compared to submergence of the nozzle for the top spray fills).

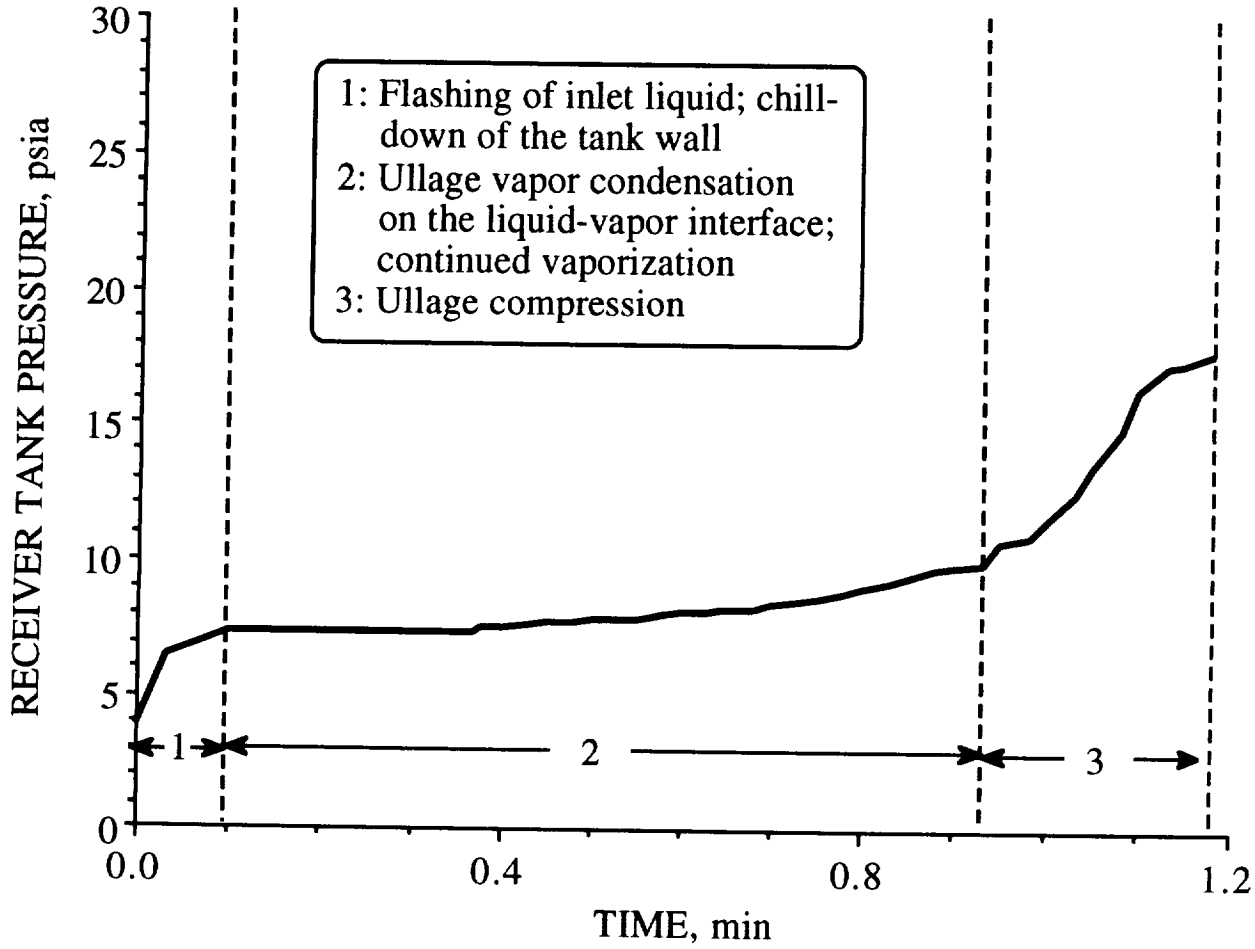

Fig. 10: Tank pressure as a function of time for a hydrogen no-vent fill test using the upward pipe discharge fill configuration (9093G).

Fig. 11 shows the fill history for the same upward pipe discharge test. Similar to the fill plot of Fig. 7, the liquid inflow is slow initially and tapers off slightly toward the end of the test. However, the liquid fill curve is relatively linear through a majority of the run. The sawtooth pattern evident in the middle region of the plot is believed to be sloshing behavior of the liquid interface caused by the upward pipe discharge configuration. This characteristic is only observed in tests with this configuration at the higher inlet flow rates.

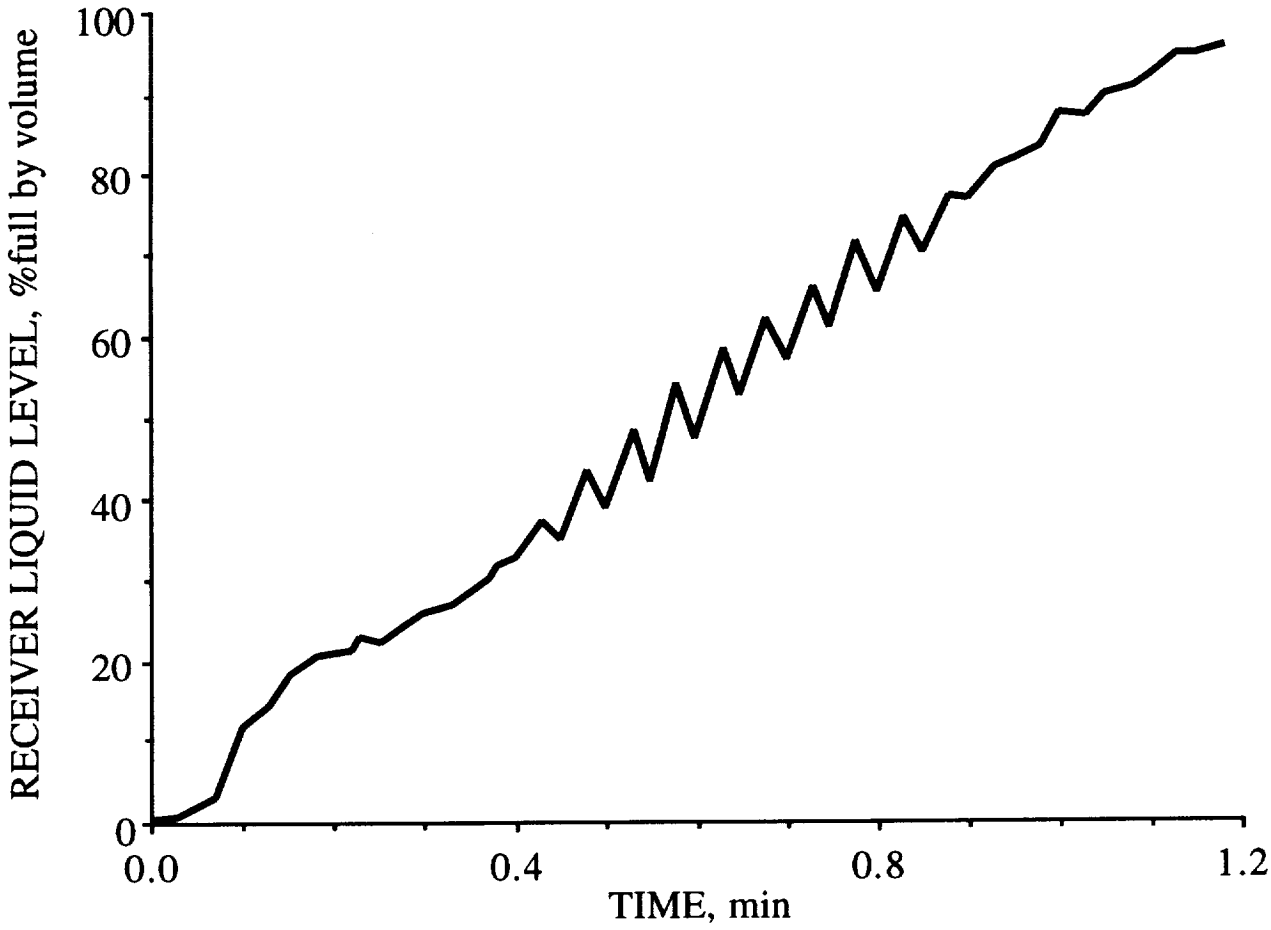

Fig. 11: Liquid fill level as a function of time for a hydrogen no-vent fill test using the upward pipe discharge configuration (9093G).

Internal tree temperatures for the same test are shown in Fig. 12. The two upper silicon diodes begin dropping in temperature rapidly in the initial moments of the fill, whereas, the lower sensors experience a sudden transitory peak in temperature and then drop to liquid hydrogen temperatures. The rapid drop shown by the top sensors indicates that the liquid is gushing to the upper portions of the tank early in the test before the pipe becomes submerged in the liquid. The behavior of the lower silicon diodes is assumed to be caused by circulation of the initially warm upper ullage vapor as the liquid is injected upward into the tank at the start of the fill. Later in the test, the uppermost sensor slowly heats up as the ullage is compressed and then cools as the interface approaches and eventually submerges the sensor.

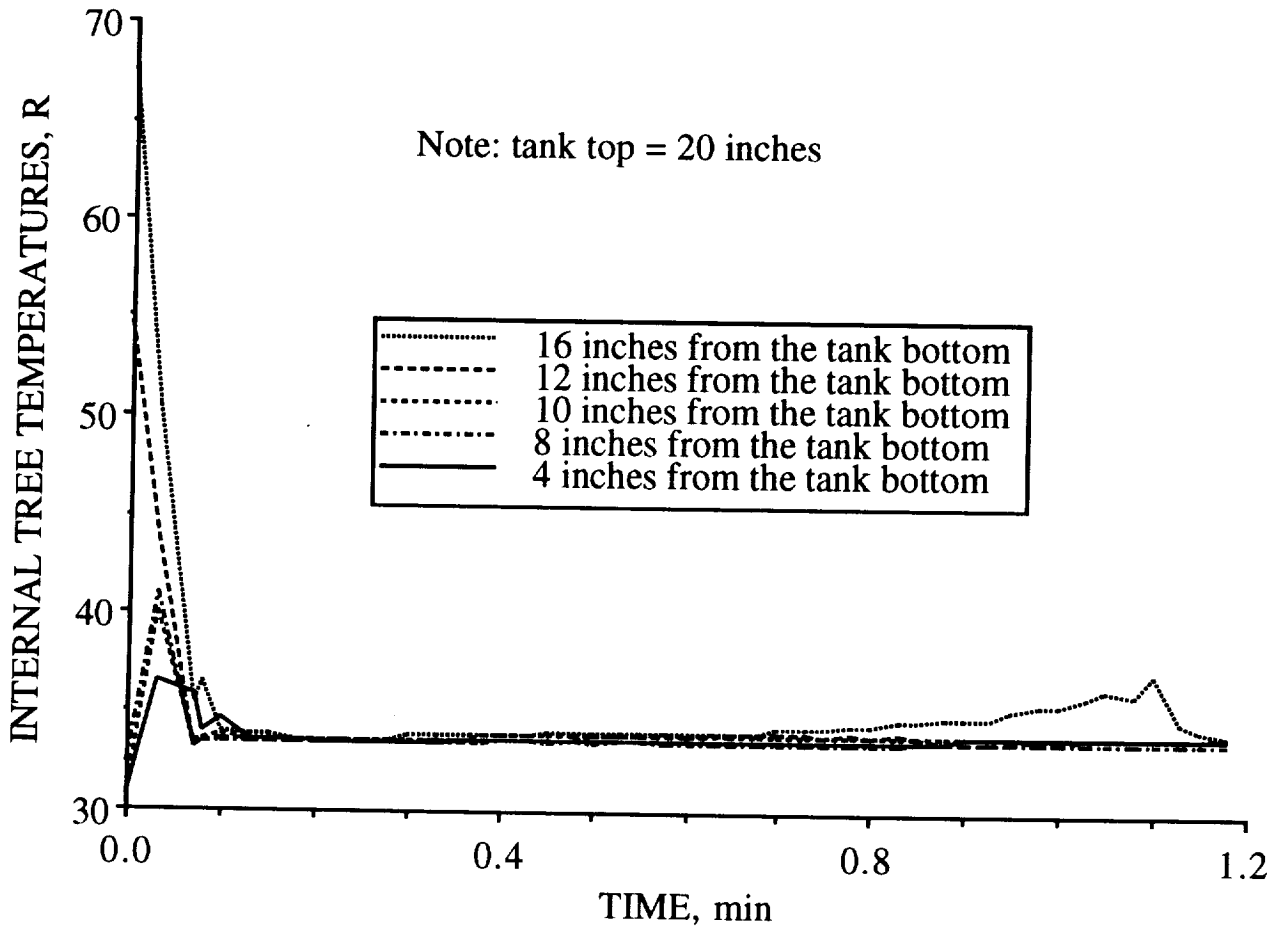

Fig. 12: Internal tree temperatures as a function of time for a hydrogen no-vent fill test using the upward pipe discharge fill configuration (9093G).

Fig. 13 displays the wall temperatures recorded during the same test. Some of the wall sensor positions have been omitted from this plot for clarity. All wall sensors cool to liquid hydrogen temperatures within the first few seconds of the test, indicating that the injected liquid fountain initially reaches the top of the tank and impinges on the side walls. As the fill progresses, the discharge opening of the pipe becomes immersed in the rising liquid. Approximately one third of the way into the run the top sensor begins to rise in temperature rapidly, coinciding with the start of the sawtooth response of the liquid level probe (see Fig. 11). This rapid temperature rise of the top wall sensor is evident in all of the upward pipe discharge tests exhibiting the sloshing behavior. The temperature rise in the top tank wall may indicate energy transfer to the ullage via slosh damping of the liquid-vapor interface. The top sensor continues to warm up more slowly during the remainder of the test due to ullage compression.

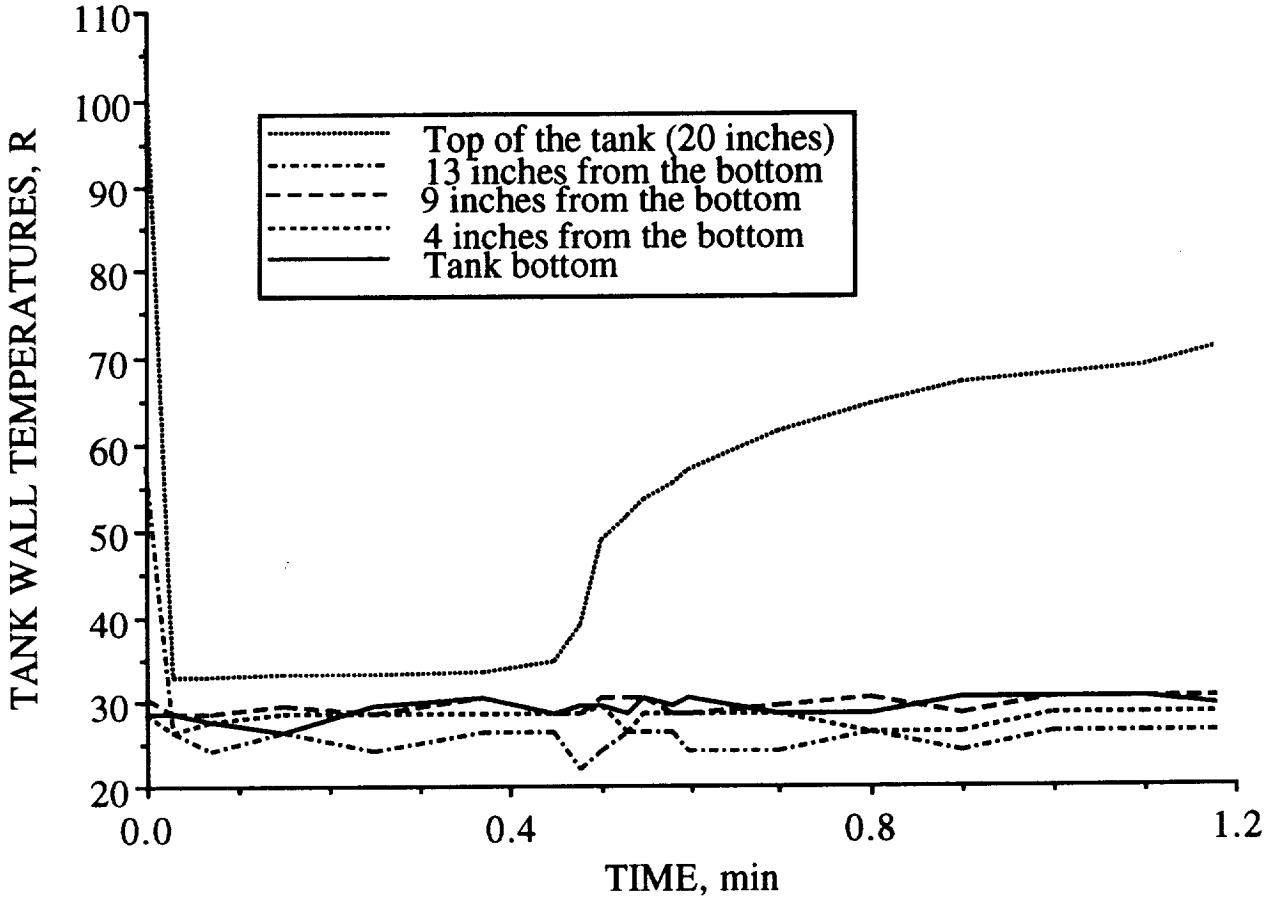

Fig. 13: Tank wall temperatures as a function of time for a hydrogen no-vent fill test using the upward pipe discharge fill configuration (9093G).

Bottom diffuser. The pressure history of one of the tests using the bottom diffuser configuration is shown in Fig. 14. No-vent fills using this injection technique do not exhibit the three pressure response regions typical of the other two fill configurations (see Figs. 6 and 10). Pressure rise at the start of this test is gradual, as the liquid is injected into the bottom of the receiver tank through a porous plug diffuser. A moderate tapering of the pressure rise in the tank is evident in the middle portion of the run with a slight increase in the pressure curve slope toward the end of the test. This fill configuration results in the smallest and most quiescent liquid interface of the three configurations tested and, therefore, the lowest condensation rate. In addition, energy from the tank wall is absorbed by the cryogen at a gradual rate as the liquid level rises in the tank.

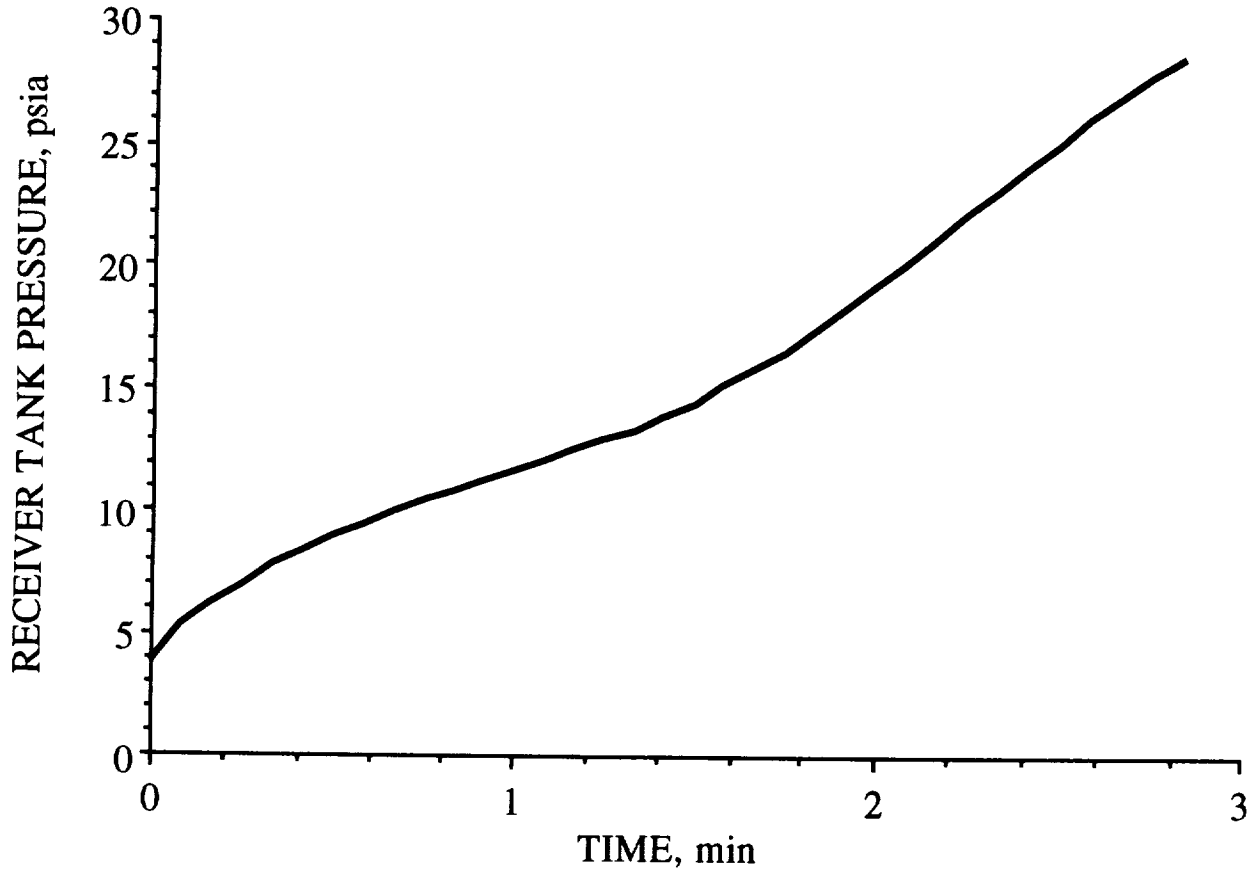

Fig. 14: Tank pressure as a function of time for a hydrogen no-vent fill test using the bottom diffuser fill configuration (9088B).

Fig. 15 shows the tank fill level as a function of time for the same test. The linear behavior of the fill level curve during most of the test indicates a nearly constant inlet flow rate. A tapering off of the liquid level rise toward the end of the test is due to the diminishing pressure difference between the supply and receiver tanks.

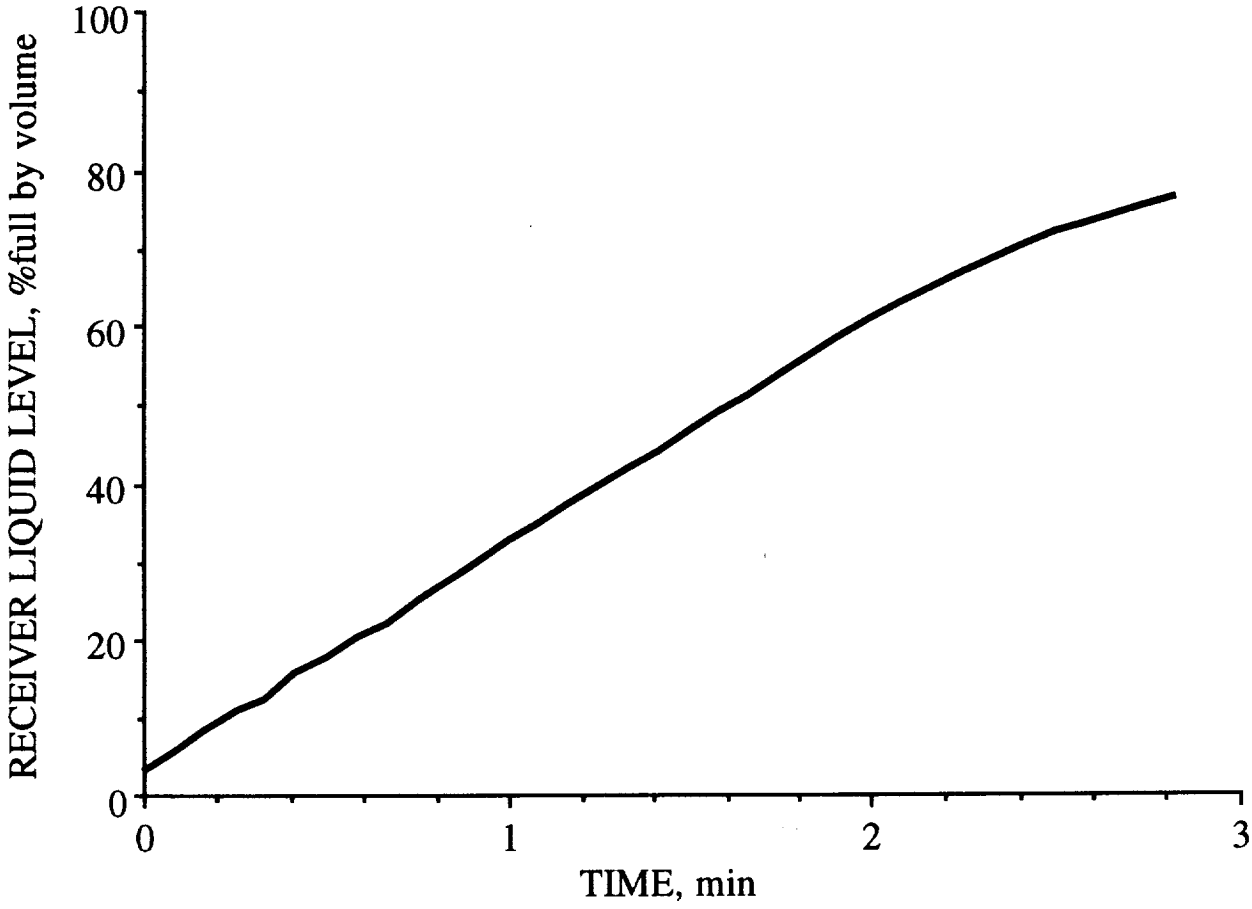

Fig. 15: Liquid fill level as a function of time for a hydrogen no-vent fill test using the bottom diffuser fill configuration (9088B).

Temperature response inside the tank during the test is shown in Fig. 16. Thermal stratification of the vapor is present at the initiation of the test, and remains throughout the run. All of the internal instrument tree sensors rise in temperature gradually until they are submerged by the liquid interface. The upper most sensor is the only one to remain in the vapor space throughout the test. Response of the internal temperatures for this configuration is markedly different than for the top spray and upward pipe discharge configurations where the tree temperatures drop rapidly at the initiation of the tests.

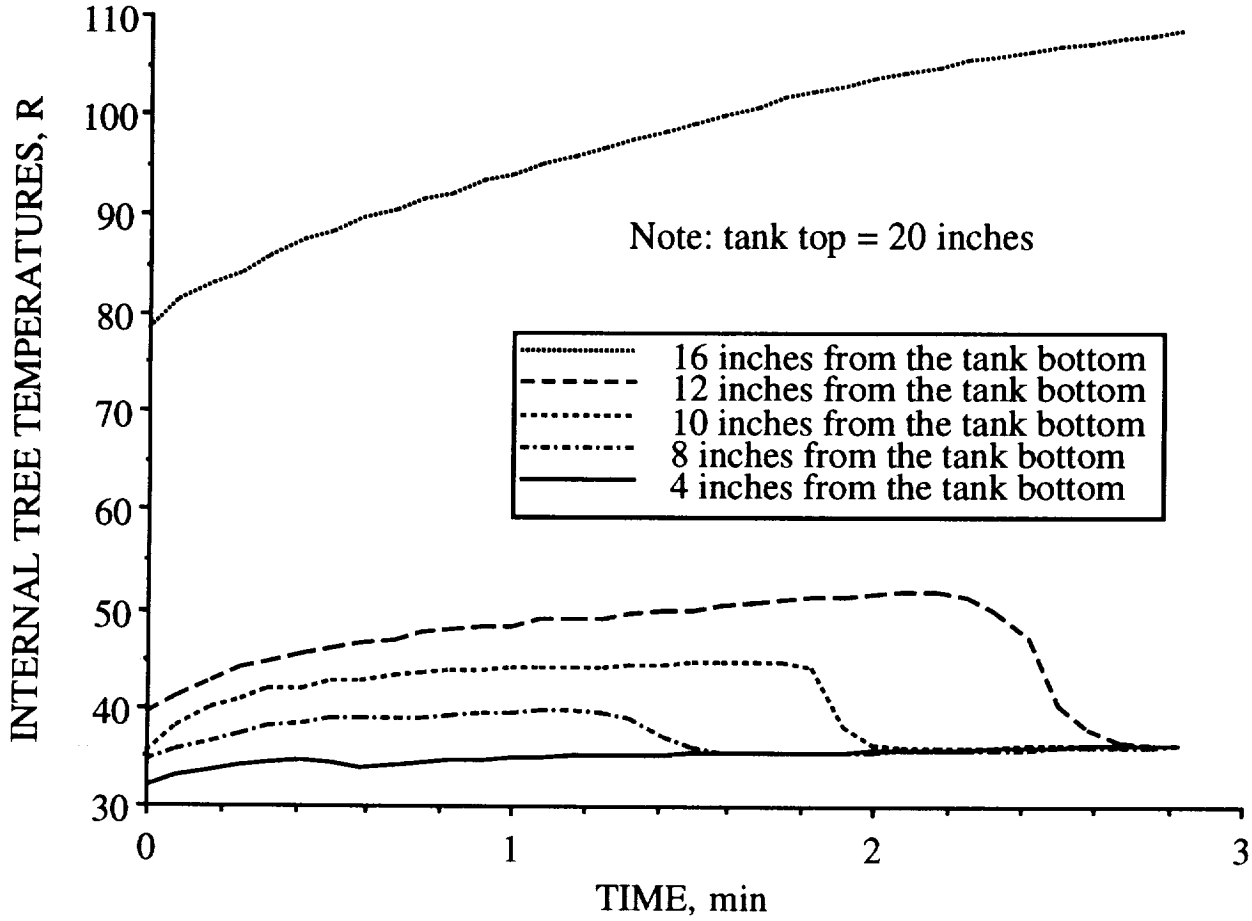

Fig. 16: Internal tree temperatures as a function of time for a hydrogen no-vent fill test using the bottom diffuser fill configuration (9088B).

Fig. 17 illustrates the tank wall temperatures recorded during the same test. Some of the wall sensor positions have been omitted from this plot for clarity. As with the internal tree temperatures, the wall sensors indicate thermal stratification in the tank at the start of the test. The stratification persists until the liquid interface passes the individual sensor locations on the tank wall. Temperature indicators in the vapor region of the tank wall continue to rise in temperature throughout the test due to ullage compression. The arrows in Fig. 17 denote where two of the thermocouple locations become submerged by the rising liquid interface.

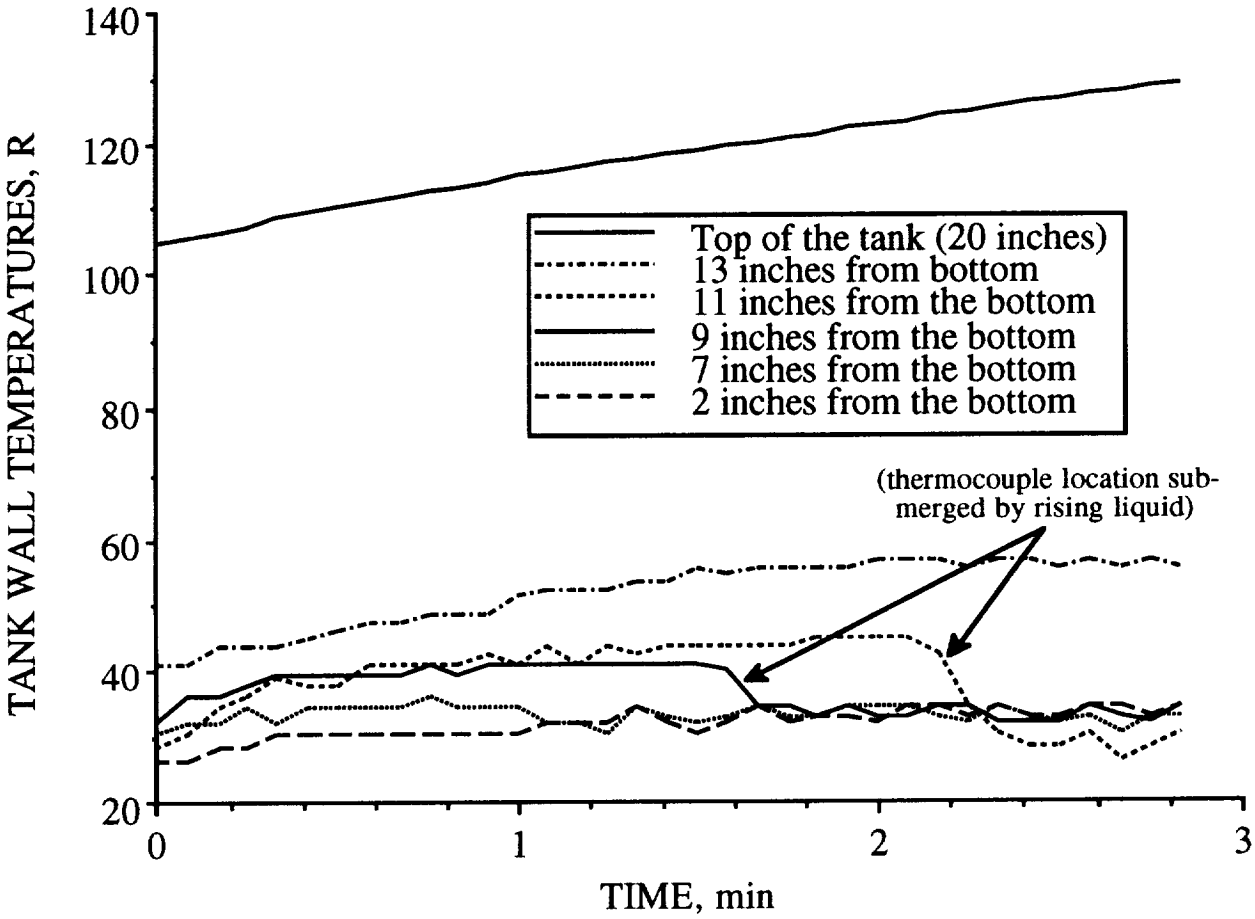

Fig. 17: Tank wall temperatures as a function of time for a hydrogen no-vent fill test using the bottom diffuser fill configuration (9088B).

Test Parameter Effects

Inlet liquid temperature. Inlet liquid temperature is one of the primary parameters effecting the tank pressure response. This effect is illustrated in Figs. 18, 19, and 20 for each of the three fill configurations. Inlet liquid temperature is measured at the venturi flowmeter located in the transfer line between the supply and small receiver tanks. The actual temperature of the liquid as it enters the receiver tank is not sensed, but it is presumed to be slightly higher than the venturi flowmeter temperature due to environmental heat leak into the transfer line. Liquid temperature rise in the transfer line from the supply tank to the venturi flowmeter was found to range from less than 1 °R to nearly 3 °R for most of the tests.

As anticipated, the pressure-versus-fill level plots indicate a lower pressure rise in the tank as the inlet temperature is decreased for all three cases. This trend was also observed in initial no-vent fill tests performed with the large receiver tank (see Ref. 1). The test runs depicted in Figs. 18 through 20 were selected to match the inlet flowrate and equivalent initial tank wall temperature as closely as possible with the widest variance of inlet temperature.

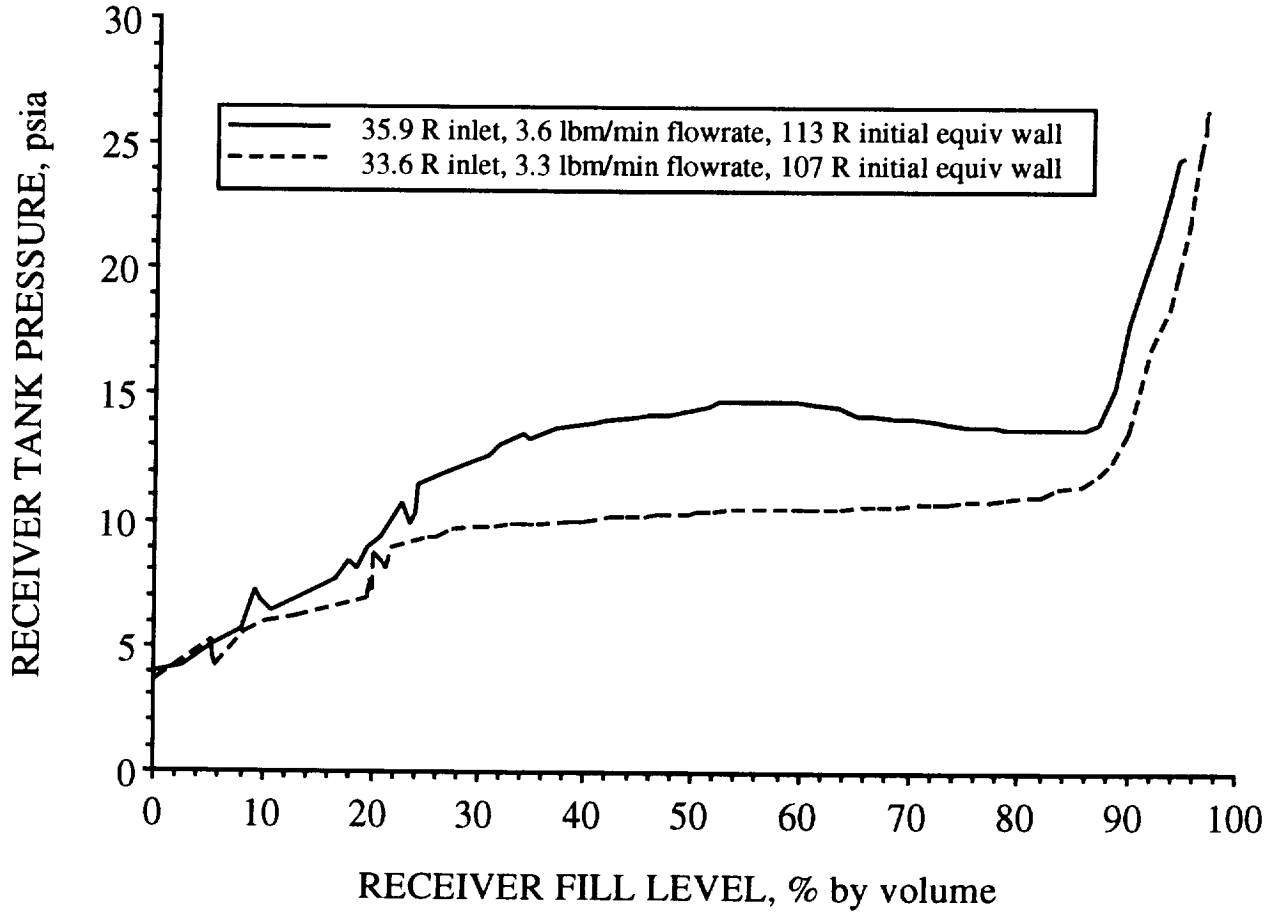

Fig. 18: Effect of inlet liquid temperature on the pressure vs. fill level response for the top spray configuration (9093C, 9094H)

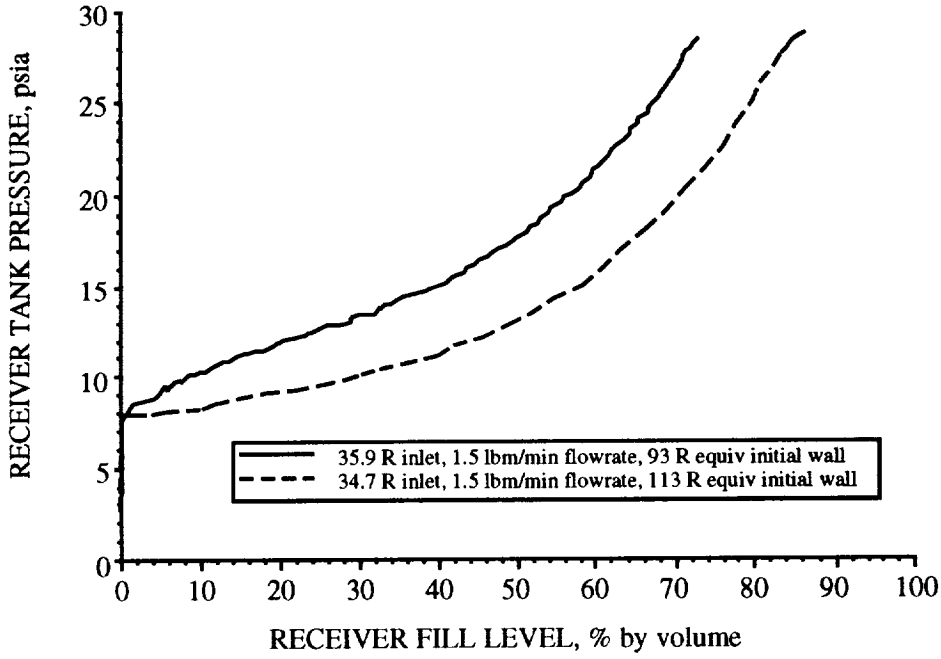

Fig. 19: Effect of inlet liquid temperature on the pressure vs. fill level response for the upward pipe discharge configuration (9093G, 9094F).

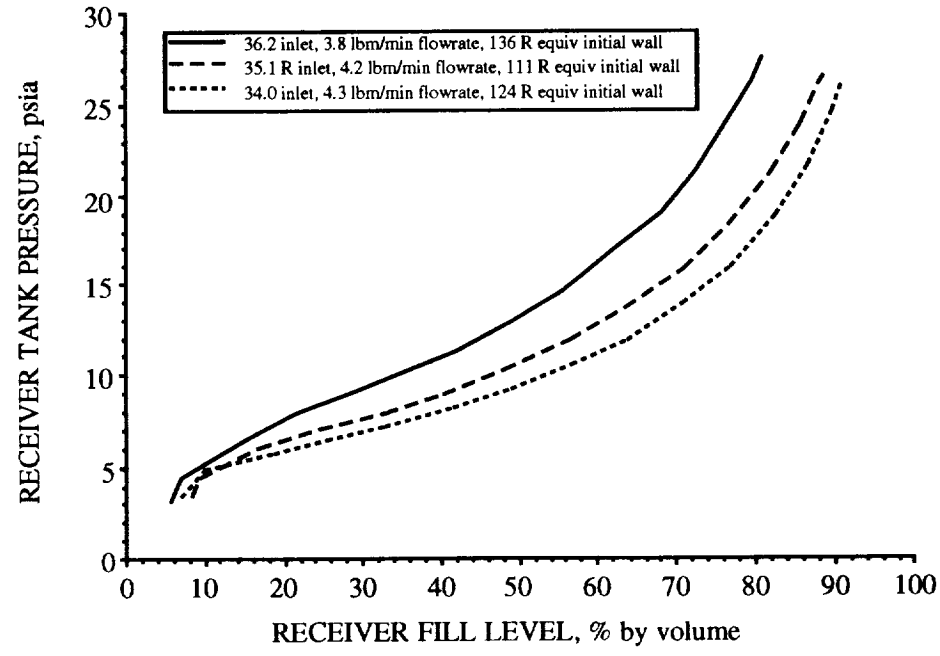

Fig. 20: Effect of inlet liquid temperature on the pressure vs. fill level response for the bottom diffuser configuration (9081G, 9088C, 9088G).

Inlet liquid flowrate. Another primary parameter is the liquid flowrate into the receiver tank. For higher flowrates, the tank pressure as a function of fill level is reduced. The liquid flowrate specified for the tests is an averaged value over the entire test run and is derived from the tank fill level data. Figures 21 through 23 illustrate this effect for all three configurations.

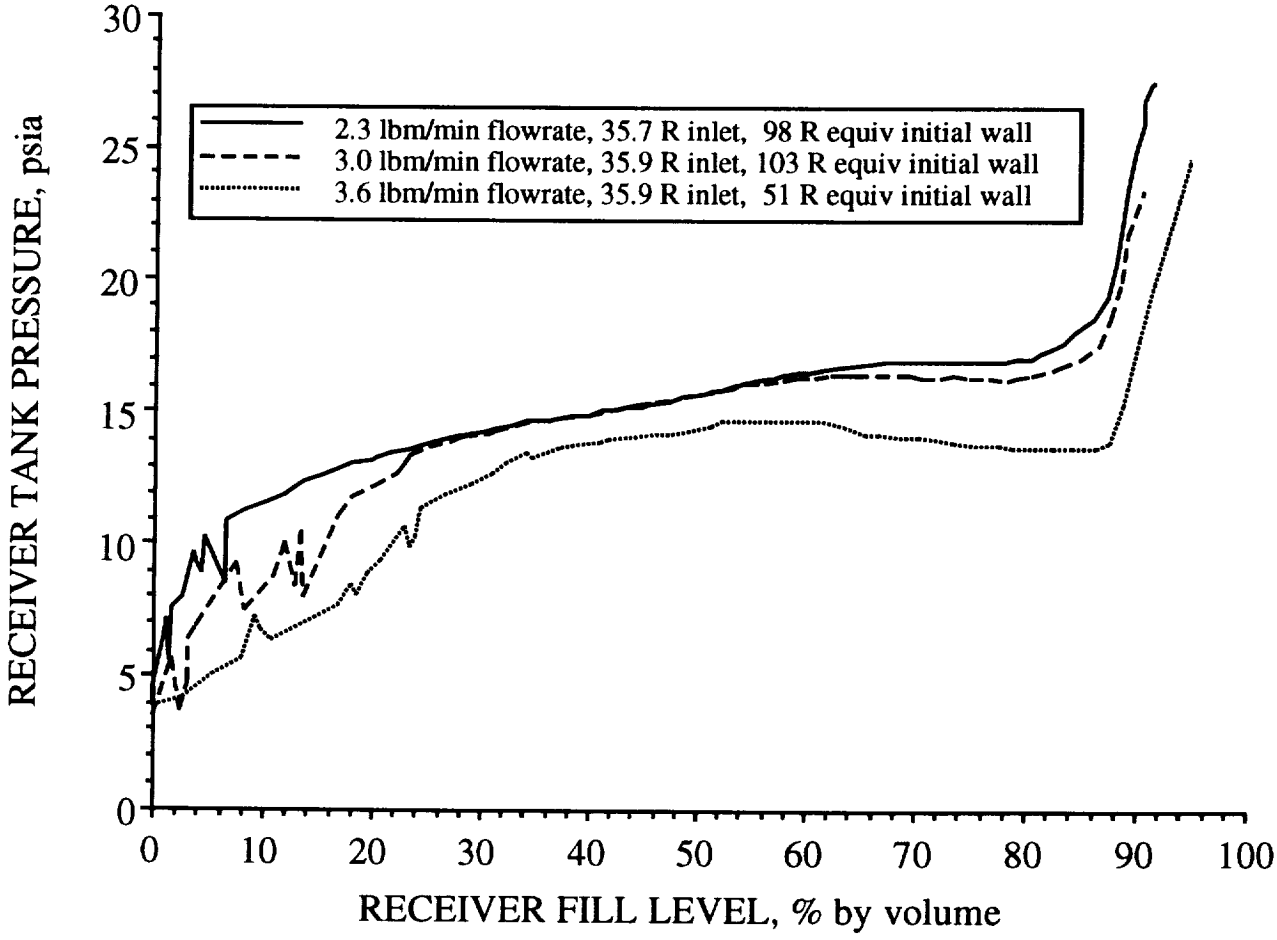

Fig. 21: Effect of inlet liquid flowrate on the pressure vs. fill level response for the top spray configuration (9094A, 9094B, 9094C).

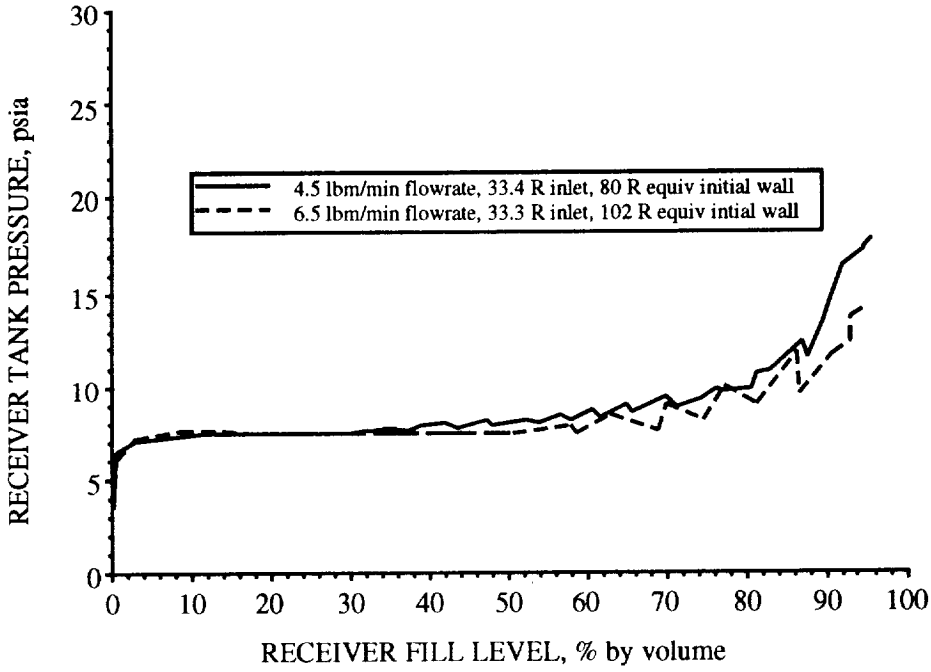

Fig. 22: Effect of inlet liquid flowrate on the pressure vs. fill level response for the upward pipe discharge configuration (9093F, 9093G).

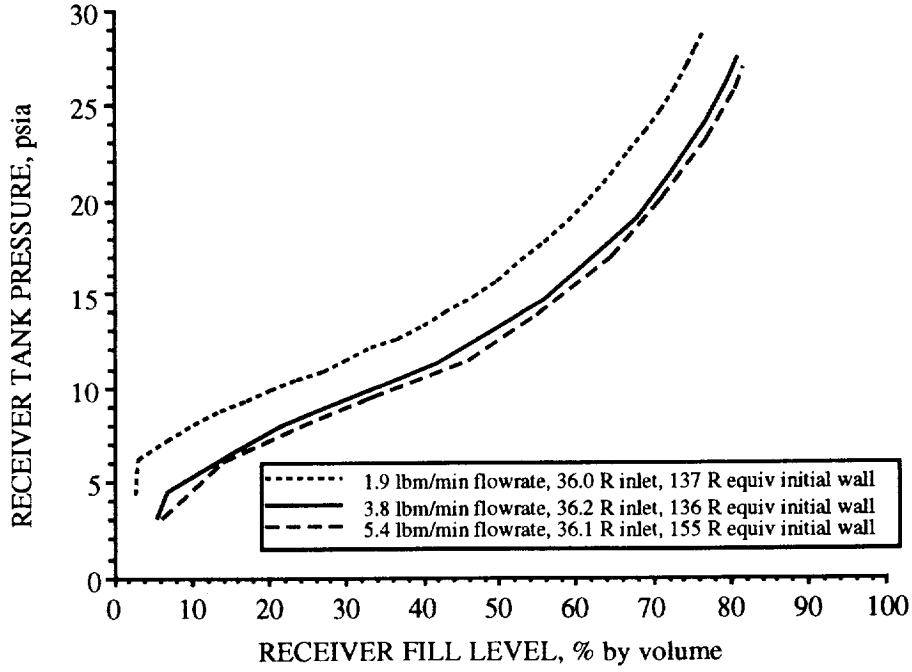

Fig. 23: Effect of inlet liquid flowrate on the pressure vs. fill level response for the bottom diffuser configuration (9075C, 9088C, 9088D).

Initial equivalent wall temperature. The effect of initial equivalent wall temperature on the pressure response was more difficult to isolate for this series of tests. Initial equivalent wall temperature is a weighted average temperature that accounts for variable wall mass and the strong temperature dependence of the specific heat of stainless steel at cryogenic temperatures. Most of the no-vent fill tests were initiated with a large temperature gradient in the tank wall (see Figs. 9, 13, and 17). Fig. 24 illustrates the variance in pressure response for two bottom diffuser tests with different equivalent initial wall temperatures and well matched inlet temperature and flowrate.

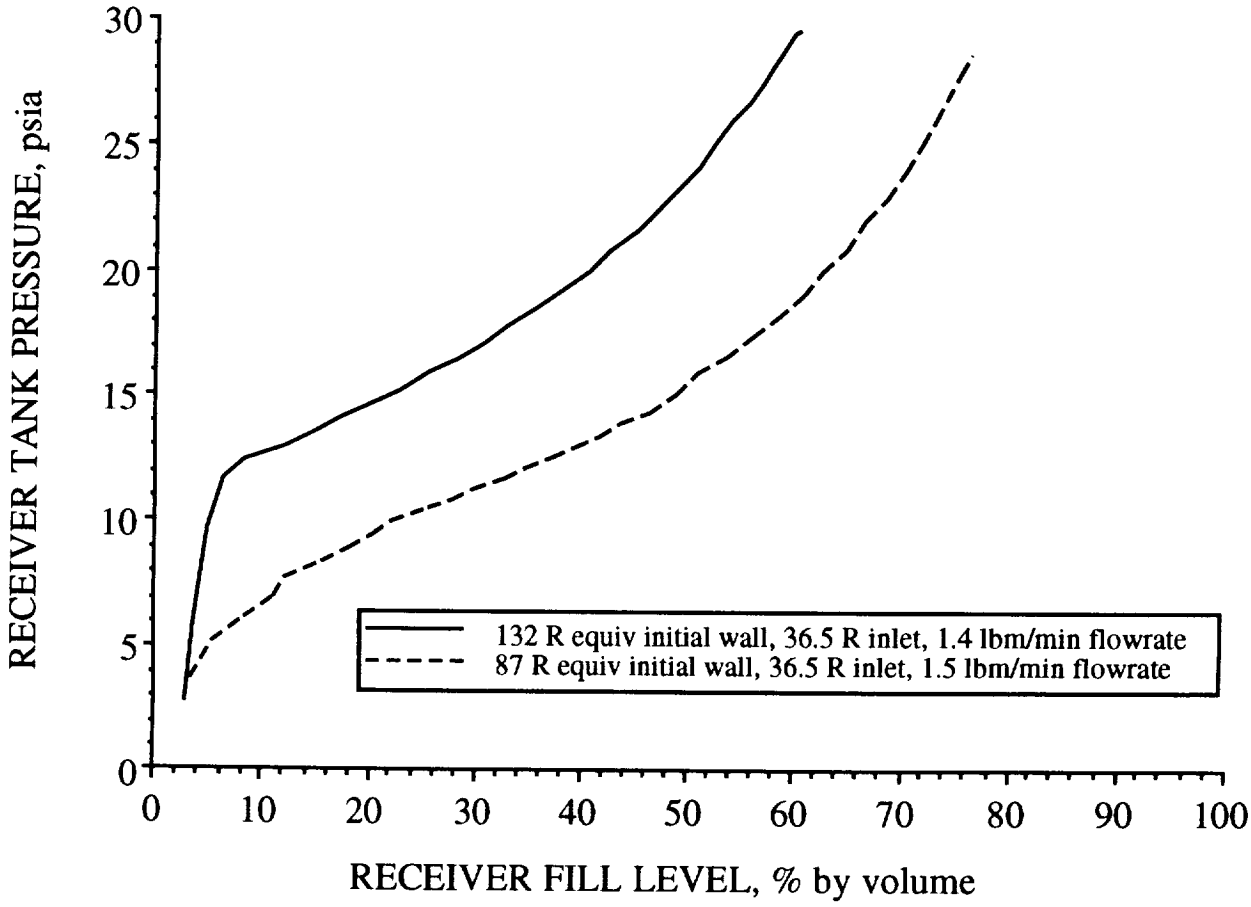

Fig. 24: Effect of equivalent initial wall temperature on the pressure vs. fill level response for the bottom diffuser configuration (9081B, 9088B).

Secondary parameters. Other secondary test parameters also effect the pressure response during a no-vent fill test. These test conditions include the initial tank wall temperature distribution, fill level-versus-time profile, and the sensible heat gain in the liquid as it flows through the transfer line. Careful attention was paid to the secondary parameters when matching test runs for comparison.

An example of the effect of these other parameters is demonstrated in Fig. 25. Two bottom diffuser configuration tests with comparable average inlet temperature and flowrate, and nearly identical initial equivalent wall temperature, exhibit significantly different pressure response. Closer examination of the test conditions for these runs, however, reveal discrepancies between both the initial tank wall temperature distribution and the fill profile for the two tests .

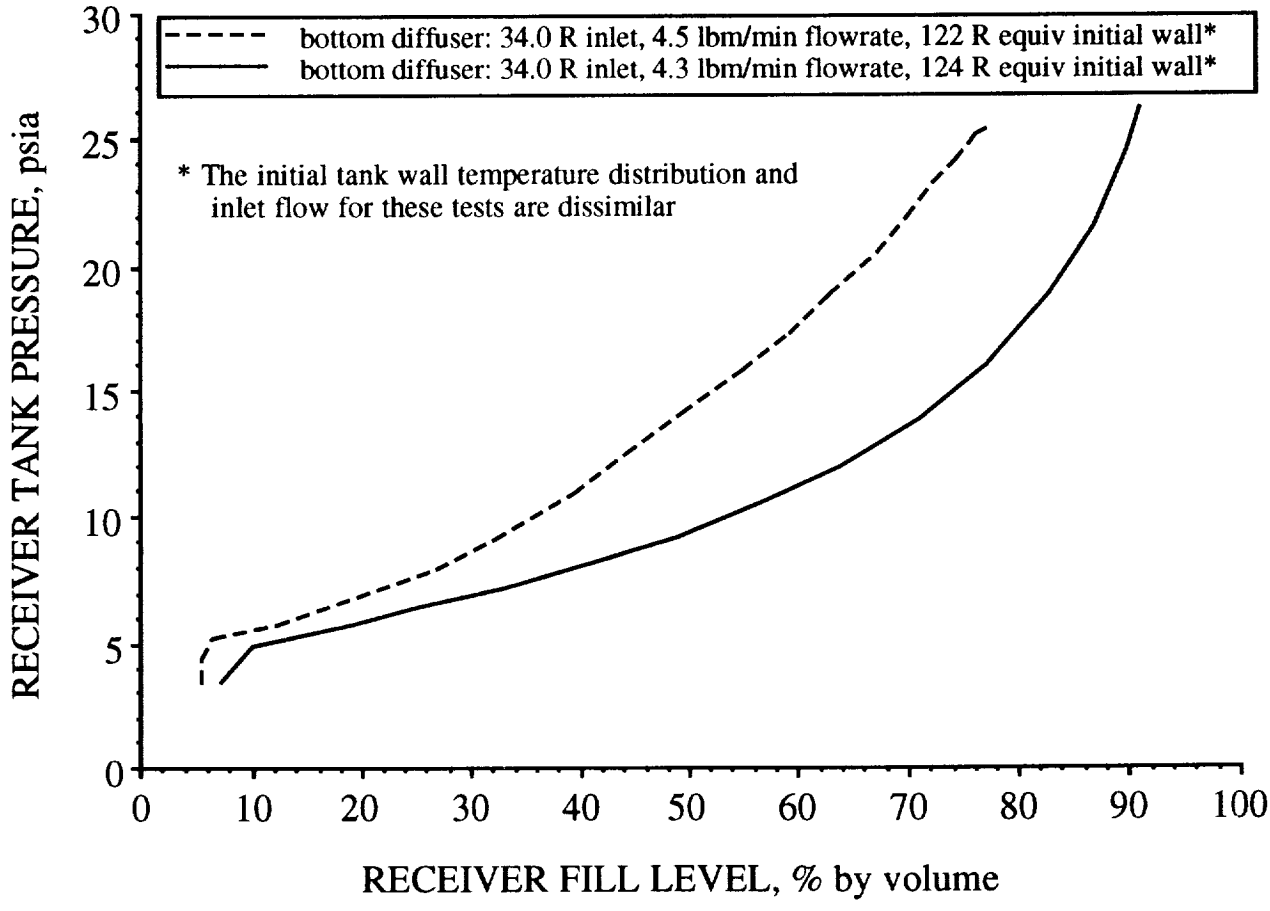

Fig. 25: Effect of secondary test parameters on the pressure vs. fill level response for the bottom diffuser configuration (9088G, 9088H).

Table I illustrates the temperature distribution for both no-vent fills at the initiation of the tests. Although the initial equivalent wall temperatures calculated for the two tests are within 2 °R of each other, the temperatures measured at discrete positions on the tank wall differ considerably. Test number 9088G has lower wall temperatures in the main body of the tank and a higher top (lid) temperature as compared to test 9088H. Since the lid of the tank represents approximately one third of the test mass of the tank, and the specific heat of stainless steel increases dramatically with increasing temperature in this range, significantly more thermal energy is stored in the tank lid for test number 9088G. For the bottom diffuser no-vent fills, the tank lid temperature tends to remain constant throughout the test while the remainder of the tank cools to liquid hydrogen temperature as the liquid level rises. Therefore, more thermal energy is removed from the tank in test 9088H by virtue of the difference in tank wall temperature distribution even though the calculated equivalent (averaged) wall temperature is virtually identical.

Table I: Initial tank wall temperatures (in °R) for two bottom diffuser tests with nearly identical initial equivalent wall temperature (9088G, 9088H).

Test	Tank Wall Position							
Number	Bottom	2 inches	4 inches	7 inches	9 inches	11 inches	13 inches	Top
9088G	36	36	39	37	42	49	55	161
9088H	37	34	37	40	52	61	77	149

The fill profile for the same two tests is shown in figure 26. Although the average inlet flowrate is similar for the two tests, the fill level profile demonstrates a discrepancy in the transient fill rate. This difference in fill rates effects the pressure response of the receiver tank over the course of the tests.

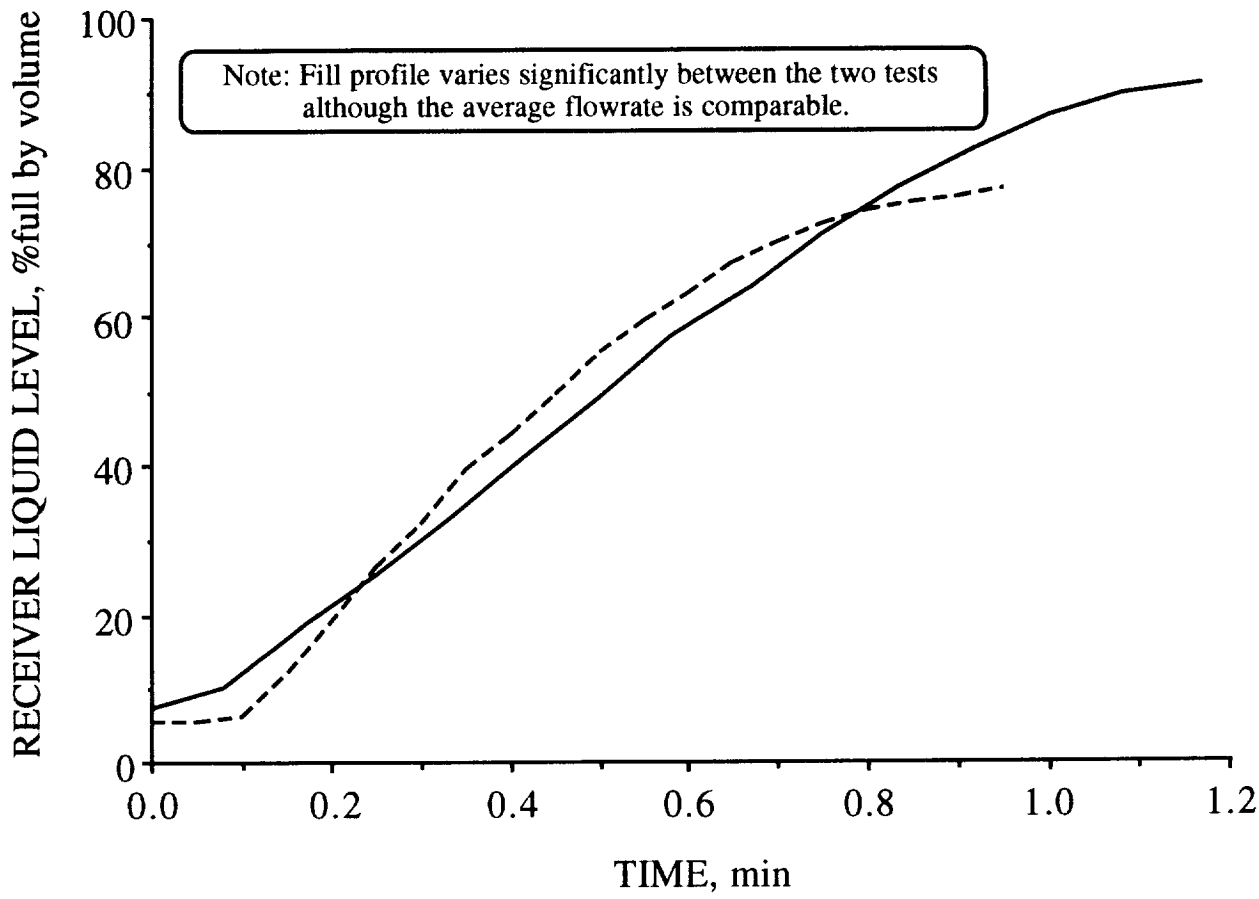

Fig. 26: Fill profile for two bottom diffuser tests with comparable average flowrate (9088G, 9088H).

Test Hardware Comparisons

Fill configuration. Direct comparisons between the three fill configurations tested are difficult to make. The various liquid injection methods result in different tank wall and internal temperature response, and diverse flowrate profiles.

A tank pressure comparison plot of an upward pipe discharge and top spray test with similar test parameters is illustrated in Fig. 27. For the upward pipe discharge configuration, an increasing pressure slope is evident throughout most of the test run. Conversely, the pressure slope for the top spray technique tapers off during the middle portion of the test, and then increases rapidly at

the end as the spray nozzle is submerged. Both tests indicate a rapid tank pressure rise at the test initiation as the cold inlet liquid impinges on the warmer tank walls. Inspection of the tank pressure at discrete fill levels from Fig. 27 shows that the upward pipe discharge configuration yields higher tank pressures for all but a small fill level range.

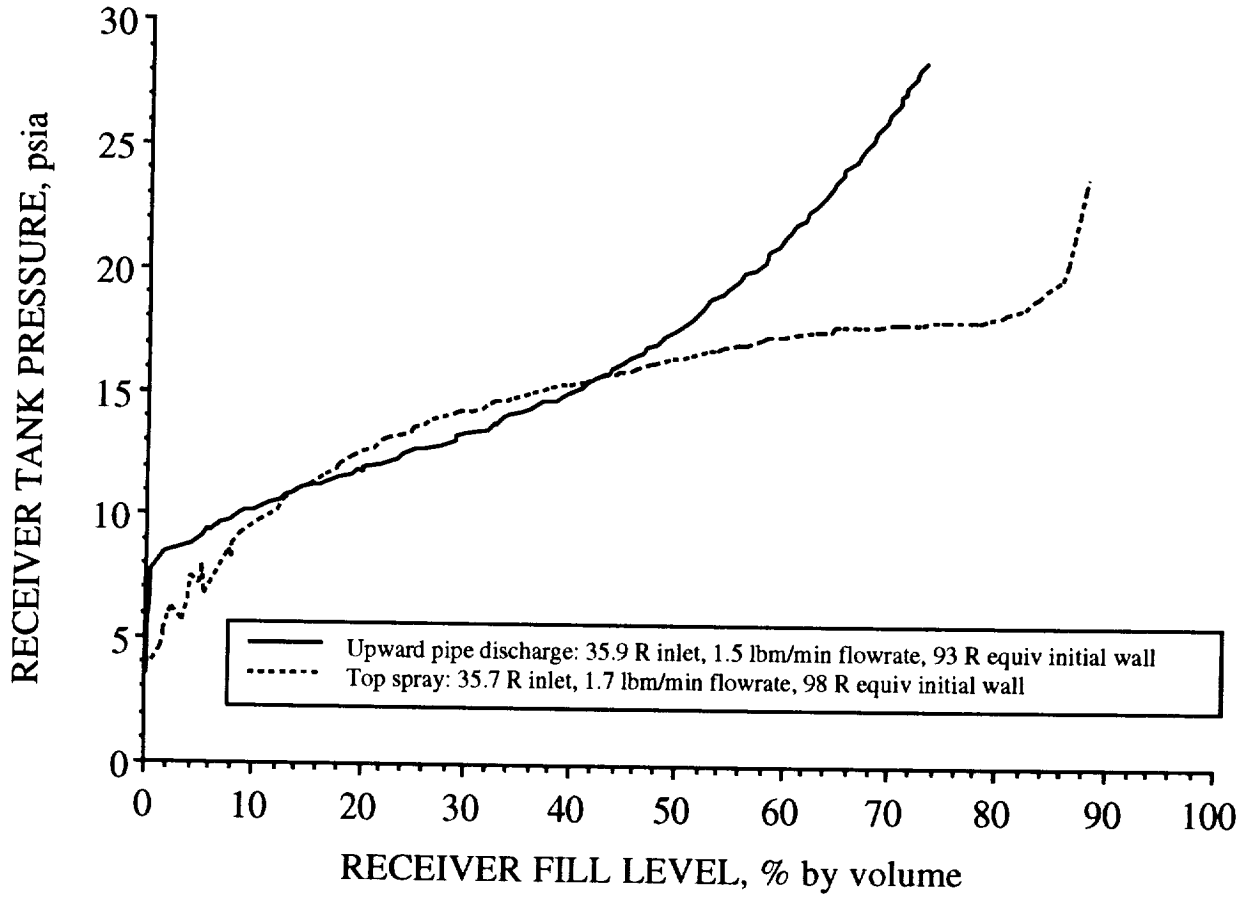

Fig. 27: Comparison of pressure response for an upward pipe discharge and a top spray test with similar test parameters (9094E, 9094D).

A similar comparison plot of a bottom diffuser and an upward pipe discharge test is given in Fig. 28. A sharp pressure rise from 2.7 to nearly 8 psia is evident for the upward pipe discharge test as the incoming liquid impinges on portions of the tank wall. Although the initial pressure rise for the downward diffuser test is less severe, it overtakes the pipe discharge test around the 30% fill level, and remains at a higher tank pressure throughout the remainder of the no-vent fill.

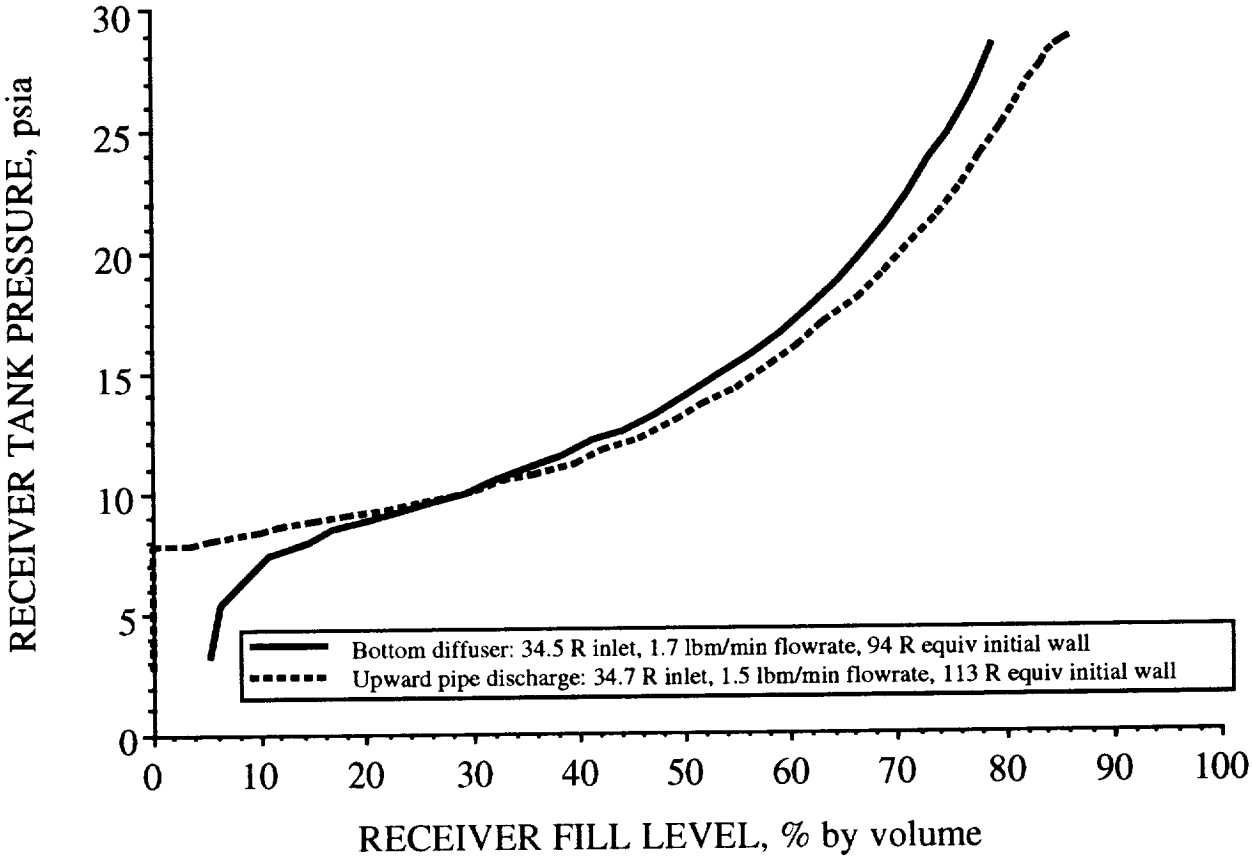

Fig. 28: Comparison of pressure response for an upward pipe discharge and a bottom diffuser test with similar test parameters (9080B, 9093E).

Receiver Tank Size (Scaling). A final comparison can be attempted between the small receiver tests and the large receiver no-vent fills previously reported (see ref. 1). The inlet flowrate and equivalent initial wall temperature must be appropriately scaled to account for the difference in tank size, whereas the inlet liquid temperature is matched directly. Scaling techniques presented in Refs. 2 and 3 were used to scale the test parameters (see Appendix B for detailed calculations). Fig. 29 illustrates the pressure response as a function of fill level for one of the large receiver no-vent fills and two small receiver tests which approximate the scaled parameters. All three tests were conducted with the top spray fill configuration.

The two small receiver tests parallel the pressure response of the large receiver no-vent fill moderately well. Referring to Fig. 29, the small receiver test that is nearer to the desired equivalent initial wall temperature (solid plot line) closely matches the initial pressure peak of the large receiver test. Conversely, the other small receiver test (dashed plot line), with an inlet liquid temperature closer to the scaled value, has a final tank pressure that is nearly identical to the large receiver test. Unfortunately, none of the tests performed with the large and small receiver tanks can be perfectly matched to the desired scaled values for the key test parameters. However, the pressure profile resemblance illustrated in Fig. 29 provides preliminary evidence that the no-vent fill process is scalable for similarly configured tanks of different capacities.

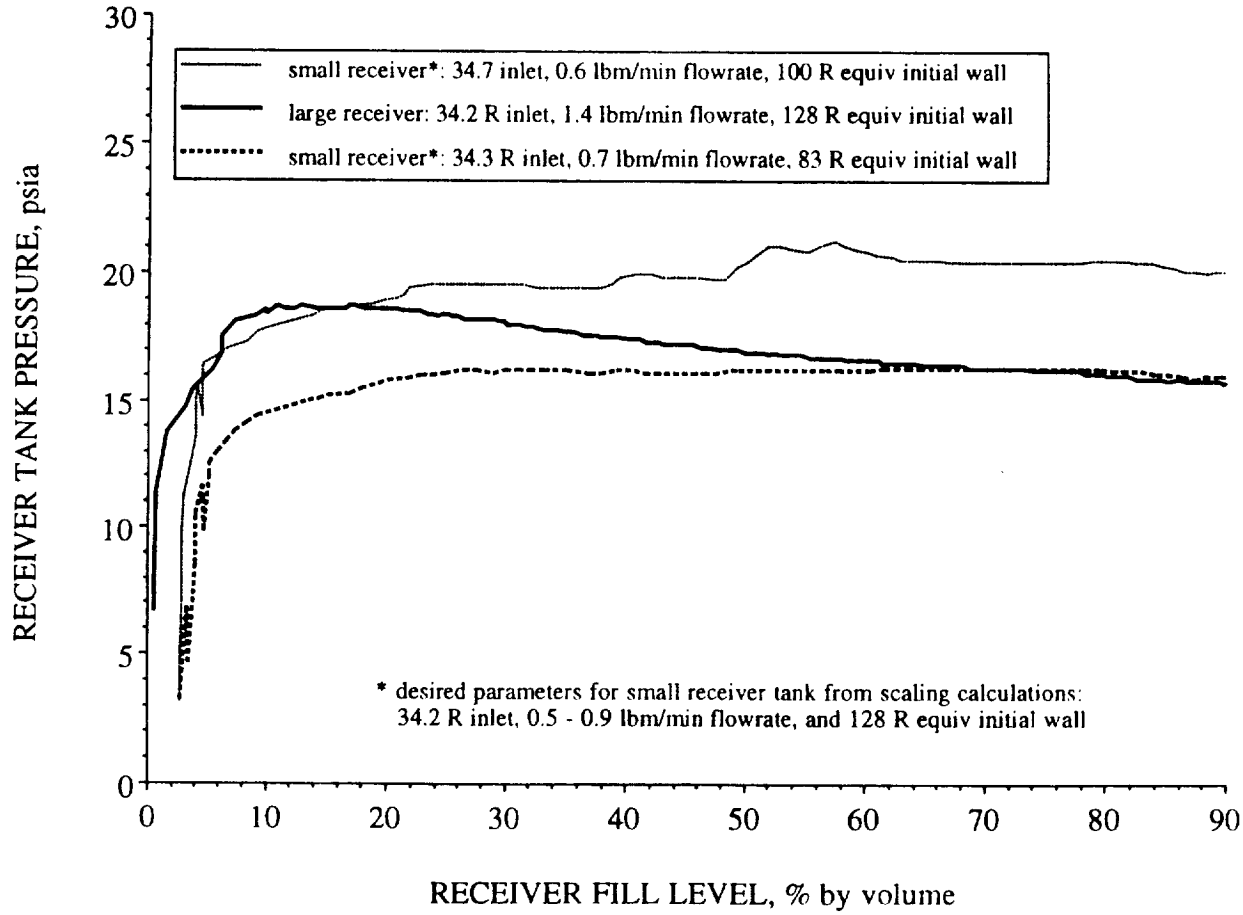

Fig. 29: Comparison of pressure response as a function of fill level for one large receiver no-vent fill, and two scaled small receiver tests (89298, 9075D).

SUMMARY OF RESULTS

A key result of the testing performed is the demonstration of the no-vent fill technique for hydrogen in a repeatable fashion under normal gravity conditions. Fill levels equal to or exceeding 90 percent by volume were achieved in approximately 40 percent of the tests with the tank pressure limited to a maximum of 30 psia. Variable test parameters and liquid injection configurations provide some insight into the conditions necessary for a successful transfer of liquid hydrogen by this method. Appendix C lists all of the hydrogen no-vent fills performed in this test series with the small (1.2 cubic foot) receiver tank along with primary initial and averaged test parameters. Analytical work being conducted with this and other test data will help to further characterize the no-vent fill process (Refs. 2 and 3)

The effect of several test parameters is illustrated by the comparison of pressure histories as a function of tank fill level for carefully selected test runs. The magnitude of the receiving tank pressure profile is found to be directly proportional to the inlet liquid temperature and equivalent initial wall temperature and indirectly proportional to the inlet liquid flowrate (i.e. higher liquid inlet and wall temperatures, and lower inlet flowrates, produce higher receiving tank pressures). Since the tank pressure is limited to a maximum value, the final fill level is indirectly proportional to the tank pressure response. Secondary test conditions such as initial tank wall temperature distribution and fill level profile as a function of time also contribute to the tank pressure response.

Fill Configuration and Scaling

Three different liquid injection techniques were employed, and each displayed unique responses in the receiver tank during the no-vent fill process. The top spray configuration, which promotes condensation of the ullage vapor onto the incoming liquid droplets, cools the tank walls rapidly early in the test and results in a steep initial pressure rise in the tank. The internal tank temperatures also cool rapidly to near saturation temperature as the spray enters the tank. As the no-vent fill process continues, the effect of ullage condensation results in a decrease in the slope of the pressure curve during much of the remaining test. This fill method yields the lowest tank pressure of the three tested configurations for comparable test conditions.

Much like the top spray, the upward pipe discharge configuration initially cools most of the tank wall and results in a similarly rapid pressure rise during the early moments of the fill. The internal tank temperatures also cool quickly. Soon after the start of the test, the outlet of the discharge pipe becomes submerged by the rising liquid interface, and condensation of the ullage vapor is limited to this surface. The bulk fluid motion induced by the pipe discharge arrangement enhances condensation at the interface as cooler fluid is circulated upward. This fill method results in a

higher tank pressure than the top spray method due, primarily, to the reduced surface area available for condensation. However, the upward pipe discharge configuration produces lower tank pressure than the bottom diffuser configuration for similar test parameters.

In contrast, the bottom diffuser injection technique cools only the lower portion of the tank wall during the initial moments of a no vent fill and results in a rather gradual pressure rise at the start of a test. Tank wall temperatures remain stratified near the starting conditions while in contact with the vapor. Portions of the wall cool rapidly when in contact with liquid hydrogen as the liquid level increases in the tank. The internal instrument tree temperatures react in a similar manner, and both the wall and internal temperatures increase gradually while in the vapor due to vapor compression. As the fill progresses, the submerged diffuser does not produce much bulk liquid motion, and the liquid near the vapor interface remains close to saturated temperature at the tank pressure. This condition results in much less condensation at the liquid-vapor interface as compared to the other two configurations and, consequently, the tank pressure rise is greater.

All three configurations demonstrate the primary importance of controlling the mass and heat transfer process at the liquid-vapor interface during a no-vent fill, and to a lesser extent, the cooldown process of the tank wall.

A final comparison is made of one of the large receiver no-vent fills and two scaled small receiver tests; all utilizing the top spray injection technique. The pressure-versus-fill level plot of the scaled small receiver runs parallel the large receiver pressure response. This similarity in pressure response lends support to the scalability of no-vent fill data to different size tanks of comparable geometry and liquid injection configuration.

CONCLUDING REMARKS

A final note regards the utility of the data presented in this report as related to on orbit or in space transfer of cryogenic propellants. The primary benefits of the ground test program are to assist in the refinement and partial validation of analytical codes for modeling the no-vent fill process, and to demonstrate concept feasibility. This work is ongoing, and preliminary comparisons of analytical versus experimental data are detailed in Refs. 4 and 5. However, complete validation of the codes and a thorough understanding of the no-vent fill process for in space use can only be accomplished with tests conducted in a low gravity environment for extended periods.

Normal gravity tests yield some indication of the effect of test parameters such as inlet liquid temperature, wall temperature, and inlet flowrate on low gravity transfers. Nevertheless, the effect of specific injection techniques and hardware configurations on the no-vent fill process cannot be reliably extracted from ground based results. This is primarily due to the lack of significant

buoyancy forces in low gravity environments, which both diminishes natural convection heat transfer, and complicates the prediction of the liquid-vapor interface location within the tank. These are key factors in the normal gravity tests conducted where, for instance, a liquid spray is injected into the ullage or the discharge of the liquid inlet pipe is directed toward the interface to promote bulk fluid circulation. In a low gravity situation the position of the liquid-vapor interface would likely be uncertain. Furthermore, the thermal gradients of the liquid and vapor in the tank would be primarily governed by conduction heat transfer for a quiescent tank, whereas natural convection plays a key role under normal gravity conditions.

For these reasons, comparison of injection techniques used in ground tests to desired hardware designs for in space use should be made with extreme caution. Of more value are the trends in tank pressure and temperature as related to the physical processes induced by the injection methods. Ultimately, testing of the effect of a number of carefully chosen configurations on the no-vent fill process under extended low gravity conditions will be needed.

APPENDIX A

NOMENCLATURE

C_p	specific heat
$\dot{M}$	inlet liquid mass flowrate
m	mass
T	temperature
V	volume
S	scale factor

Subscripts

i	initial
f	final
lr	large receiver tank
sr	small receiver tank
t	tank

APPENDIX B

SCALING CALCULATIONS

In order to compare no-vent fill tests conducted in the large and small receiver tanks, previously published scaling relations (Refs. 2 and 3) were utilized to scale the equivalent initial tank wall temperature and inlet liquid flowrate.

Equivalent Initial Tank Wall Temperature

From Ref. 2 (eqn. 13), if two tanks are constructed of the same material and contain the same fluid, then a relation based on thermodynamic similarity can be written as,

$$\left(\int_{T_f}^{T_i} C_{pt}\, dT_t\right)_{sr} = \frac{V_{t,sr}}{V_{t,lr}}\,\frac{m_{t,lr}}{m_{t,sr}}\left(\int_{T_f}^{T_i} C_{pt}\, dT_t\right)_{lr}$$

Substituting for the large and small receiver tank volumes and masses in equation (1) yields,

$$\left(\int_{T_f}^{T_i} C_{pt}\, dT_t\right)_{sr} = \left(\frac{2107\ in^3}{8773\ in^3}\right)\left(\frac{30.45\ lbm}{7.89\ lbm}\right)\left(\int_{T_f}^{T_i} C_{pt}\, dT_t\right)_{lr} = 0.927\left(\int_{T_f}^{T_i} C_{pt}\, dT_t\right)_{lr} \qquad (2)$$

The specific heat of the stainless steel tank wall can be closely approximated in the temperature range of 36 °R to 360 °R by the expression,

$$C_{pt} \cong 0.0689 - 0.0227\ T^{1/2} + 0.00197\ T - 1.92\text{x}10^{-6}\ T^2 \quad \left(\frac{Btu}{lbm\cdot{}^\circ R}\right) \qquad (3)$$

Therefore,

$$\int_{T_f}^{T_i} C_{pt}\, dT_t \cong \left| 0.0689\ T - 0.0151\ T^{3/2} + 9.85\text{x}10^{-4}\ T^2 - 6.40\text{x}10^{-7}\ T^3 \right|_{T_f}^{T_i} \quad \left(\frac{Btu}{lbm}\right) \qquad (4)$$

Substituting the initial and final tank wall temperatures from large receiver no-vent fill number 89298 (test H2 in Ref. 1) into equation (4) results in,

$$\left(\int_{T_f}^{T_i} C_{pt}\, dT_t\right)_{lr} = 1.748 - 0.477 = 1.271 \qquad (5)$$

for T_i = 128 °R and T_f = 44 °R.

Incorporating this result into the right side of equation (2) yields,

$$\left(\int_{T_f}^{T_i} C_{pt}\, dT_t \right)_{sr} = 0.927\ (1.271) = 1.178 \tag{6}$$

Inspection of the small receiver no-vent fills reveals that most of the tests have a final tank temperature near 70 °R for the top spray configuration. Assuming this value for the small receiver final tank temperature, equation (6) is solved numerically for T_i to obtain,

$$T_i = 128.5\ ^\circ R \tag{7}$$

This temperature is the desired equivalent initial wall temperature for the small receiver tank to appropriately scale the large receiver no-vent fill test number 89298. Because the receiver tanks are similarly constructed, the scaled initial tank temperature for the small receiver tank is nearly identical to the actual initial temperature of the large receiver tank. This trend is true for all of the large receiver no-vent fill tests.

Inlet Liquid Flowrate

A geometrical scale factor for similarly shaped tanks (i.e. the large and small receiver tanks) can be defined from Ref. 3 (equation 12) as,

$$S = \left(\frac{V_{sr}}{V_{lr}} \right)^{1/3} = \left(\frac{2107}{8773} \right)^{1/3} = 0.622 \tag{8}$$

For a highly mixed fill condition where the heat transfer coefficient asymptotically approaches a maximum value, Ref. 3 scales the inlet liquid flowrate by,

$$\dot{M}_{sr} = S^2\, \dot{M}_{lr} \tag{9}$$

For no-vent fill conditions where a large degree of thermal stratification exists, an alternate scaling relation is suggested (Ref. 3),

$$\dot{M}_{sr} = S\,\dot{M}_{lr} \tag{10}$$

Equations (9) and (10) provide a desired inlet flowrate range for scaling between the large and small receiver tanks. Applying these equations to large receiver no-vent fill test number 89298 ($\dot{M}_{lr}$ = 1.4 lbm/min) yields a scaled inlet flowrate range of,

$$\dot{M}_{sr} = 0.5 - 0.9 \quad \left(\frac{\text{lbm}}{\text{min}}\right) \tag{11}$$

APPENDIX C

INITIAL AND AVERAGED TEST PARAMETERS FOR HYDROGEN NO-VENT FILL TESTS WITH THE SMALL RECEIVER TANK

Fill Config;[1] Test Number	Inlet Venturi Temperature (^{O}R)	Supply Tank Liquid Temp (^{O}R)	Temperature Difference[2] (^{O}R)	Equiv Initial Wall Temp (^{O}R)	Inlet Flow (lbm/min)	Initial Tank Pressure (psia)	Pressure @ 90% full[3] (psia)	Final Fill level (% by vol)
BD; 9088G	34.0	32.5	1.5	124	4.3	3.4	25	91
BD; 9088H	34.0	32.5	1.5	122	4.5	3.4	25	77
BD; 9080D	34.4	32.4	2.0	105	5.3	3.1	26	88
BD; 9080B	34.5	32.2	2.3	94	1.7	3.2	28	79
BD; 9088F	34.6	32.5	2.1	65	1.6	4.0	30	78
BD; 9080C	34.9	32.5	2.4	63	3.5	5.2	28	67
BD; 9081G	35.1	33.3	1.8	111	4.2	3.3	27	89
BD; 9081H	35.4	33.6	1.8	157	5.5	3.4	27	82
BD; 9081C	35.8	35.1	0.7	130	3.5	2.6	26	79
BD; 9081D	36.0	34.3	1.7	114	5.4	3.3	27	82
BD; 9075C	36.0	35.1	0.9	137	1.9	4.3	29	77
BD; 9088D	36.1	35.1	1.0	155	5.4	3.1	27	82
BD; 9088C	36.2	35.1	1.1	136	3.8	3.0	28	81
BD; 9088B	36.5	35.1	1.4	87	1.5	3.7	29	76
BD; 9081B	36.5	35.2	1.3	132	1.4	2.7	30	60
BD; 9081F	37.6	33.4	4.2	154	1.0	2.7	29	29
UP; 9094I	32.8	31.6	1.2	138	6.3	3.7	16	95
UP; 9093F	33.3	32.4	0.9	102	6.5	3.4	11	95
UP; 9093G	33.4	32.4	1.0	80	4.5	3.8	14	96
UP; 9093E	34.7	32.4	2.3	113	1.5	2.7	29	87
UP; 9094F	35.1	34.3	0.8	131	4.2	3.4	27	89
UP; 9094G	35.6	34.5	1.1	99	5.2	2.9	20	94
UP; 9094E	35.9	34.3	1.6	93	1.5	3.5	28	73

Fill Config;[1] Test Number	Inlet Venturi Temperature (^{o}R)	Supply Tank Liquid Temp (^{o}R)	Temperature Difference[2] (^{o}R)	Equiv Initial Wall Temp (^{o}R)	Inlet Flow (lbm/min)	Initial Tank Pressure (psia)	Pressure @ 90% full[3] (psia)	Final Fill level (% by vol)
TS; 9094H	32.8	31.1	1.7	86	3.8	5.4	10	96
TS; 9093D	33.2	32.4	0.8	99	3.8	4.0	10	99
TS; 9093C	33.6	32.5	1.1	107	3.3	3.6	14	97
TS; 9093B	33.7	32.5	1.2	84	2.8	3.6	11	99
TS; 9093A	33.7	32.3	1.4	128	2.0	3.9	15	98
TS; 9081E	34.1	32.9	1.2	67	0.6	3.9	17	96
TS; 9072B	34.3	32.5	1.8	83	0.7	3.2	16	98
TS; 9075D	34.7	33.8	0.9	100	0.6	3.1	20	94
TS; 9088E	34.9	32.2	2.7	74	0.8	3.8	17	99
TS; 9080A	34.9	31.6	3.3	56	0.7	4.6	18	98
TS; 9094D	35.7	34.4	1.3	98	1.7	4.0	24	88
TS; 9094C	35.7	34.5	1.2	98	2.3	3.9	25	91
TS; 9094A	35.9	34.5	1.4	113	3.6	3.9	17	95
TS; 9094B	35.9	34.7	1.2	103	3.0	3.5	23	90
TS; 9072A	36.4	35.4	1.0	114	0.3	3.0	29	8
TS; 9088A	37.1	34.7	2.4	80	0.6	3.8	28	54
TS; 9075B	37.4	34.2	3.2	81	0.6	3.1	29	67
TS; 9081A	37.6	34.9	2.7	64	0.6	3.6	28	50
TS; 9075A	39.2	33.8	5.4	132	0.3	2.9	29	10

[1] Fill configurations: BD - bottom diffuser; UP - upward pipe discharge; TS - top spray.

[2] Temperature difference measured between the liquid in the supply tank and the venturi flowmeter located in the transfer line between the tanks.

[3] Receiver tank pressure when the 90% fill level was reached; or the final pressure for tests not reaching the 90% fill level.

REFERENCES

1. Moran, M.E., Nyland, T.W., and Papell, S.S., "Liquid Transfer Cryogenic Test Facility - Initial Hydrogen and Nitrogen No-Vent Fill Data", NASA TM-102572, March, 1990.

2. DeFelice, D.M., and Aydelott, J.C., "Thermodynamic Analysis and Subscale Modeling of Space-Based Orbit Transfer Vehicle Cryogenic Propellant Resupply", NASA TM-89921, 23rd Joint Propulsion Conference, AIAA-87-1764, June 29-July 2, 1987.

3. Chato, D.J., "Analysis of the Nonvented Fill of a 4.96-Cubic-Meter Lightweight Liquid Hydrogen Tank", NASA TM-102039, 27th National Heat Transfer Conference, August 5-8, 1989.

4. Chato, D.J., Moran, M.E., and Nyland, T.W., "Initial Experimentation on the Nonvented Fill of a 0.14 m^3 (5 ft^3) Dewar With Nitrogen and Hydrogen", NASA TM-103155, 5th Joint Thermophysics and Heat Transfer Conference, AIAA-90-1681, June 18-20, 1990.

5. Taylor, W.J., and Chato, D.J., "Improved Thermodynamic Modelling of the No-Vent Fill Process and Correlation With Experimental Data", 26th Thermophysics Conference, Honolulu, Hawaii, June 24-27, 1991.

REPORT DOCUMENTATION PAGE

Form Approved
OMB No. 0704-0188

1. AGENCY USE ONLY (*Leave blank*)	2. REPORT DATE	3. REPORT TYPE AND DATES COVERED
	October 1991	Technical Memorandum

4. TITLE AND SUBTITLE

Hydrogen No-Vent Fill Testing in a 1.2 Cubic Foot (34 Liter) Tank

5. FUNDING NUMBERS

WU-593-21-41

6. AUTHOR(S)

Matthew E. Moran, Ted W. Nyland, and Susan L. Driscoll

7. PERFORMING ORGANIZATION NAME(S) AND ADDRESS(ES)

National Aeronautics and Space Administration
Lewis Research Center
Cleveland, Ohio 44135 - 3191

8. PERFORMING ORGANIZATION REPORT NUMBER

E-6596

9. SPONSORING/MONITORING AGENCY NAMES(S) AND ADDRESS(ES)

National Aeronautics and Space Administration
Washington, D.C. 20546 - 0001

10. SPONSORING/MONITORING AGENCY REPORT NUMBER

NASA TM-105273

11. SUPPLEMENTARY NOTES

Matthew E. Moran and Ted W. Nyland, NASA Lewis Research Center; Susan L. Driscoll, NASA Marshall Space Flight Center, Huntsville, Alabama 35812. Responsible person, Matthew E. Moran, (216) 433-2576.

12a. DISTRIBUTION/AVAILABILITY STATEMENT

Unclassified - Unlimited
Subject Category 34

12b. DISTRIBUTION CODE

13. ABSTRACT ***(Maximum 200 words)***

Experimental results of no-vent fill testing with liquid hydrogen in a 1.2 cubic foot (34 liter) stainless steel tank are presented. More than 40 tests were performed with various liquid inlet temperatures, inlet flowrates, initial tank wall temperatures, and liquid injection techniques. Fill levels equal to or exceeding 90 percent by volume were achieved in 40 percent of the tests with the tank pressure limited to a maximum of 30 psia. Three liquid injection techniques were employed; top spray, upward pipe discharge, and bottom diffuser. Effects of each of the varied parameters on the tank pressure history and final fill level are evaluated. The final fill level is found to be indirectly proportional to the initial wall and inlet liquid temperatures and directly proportional to the inlet liquid flowrate. Furthermore, the top spray is the most efficient no-vent fill method of the three configurations examined. The success of this injection method is primarily due to condensation of the ullage vapor onto the incoming liquid droplets. Ullage condensation counteracts the tank pressure rise resulting from energy exchange between the fluid and the warmer tank walls, and ullage compression. Upward pipe discharge from the tank bottom is the next most efficient method. Fluid circulation induced by this fill configuration tends to diminish thermal stratification in the bulk liquid, thus enhancing condensation at the liquid-gas interface.

14. SUBJECT TERMS

Cryogenics; Liquid propellants; Spacecraft propulsion

15. NUMBER OF PAGES

42

16. PRICE CODE

A03

17. SECURITY CLASSIFICATION OF REPORT	18. SECURITY CLASSIFICATION OF THIS PAGE	19. SECURITY CLASSIFICATION OF ABSTRACT	20. LIMITATION OF ABSTRACT
Unclassified	Unclassified	Unclassified	